
Appendix H

Model Description for the Sacramento River Winter-run Chinook Salmon Life Cycle Model

Model Description for the Sacramento River Winter-run Chinook Salmon Life Cycle Model

Noble Hendrix¹
Eva Jennings²
Anne Criss^{3,4}
Eric Danner^{3,4}
Vamsi Sridharan^{3,4}
Correigh M. Greene⁵
Hiroo Imaki⁵
Steven T. Lindley^{3,4}

¹QEDA Consulting, LLC
4007 Densmore Ave N
Seattle, WA 98103

²Cheva Consulting
4106 Aikins Ave SW
Seattle, WA 98116

³Institute of Marine Sciences
University of California, Santa Cruz
1156 High St
Santa Cruz, CA 95064

⁴National Marine Fisheries Service
Southwest Fisheries Science Center
Fisheries Ecology Division
110 McAllister Way
Santa Cruz, CA 95060

⁵National Marine Fisheries Service
Northwest Fisheries Science Center
2725 Montlake Blvd. East
Seattle, WA 98112-2097

March 8, 2017

I. Background and Model Structure

Given the goals of improving the reliability of water supply and improving the ecosystem health in California's Central Valley, NMFS-SWFSC is developing simulation models to evaluate the potential effects of water project operations and habitat restoration on the dynamics of Chinook salmon populations in the Central Valley. These life cycle models (LCMs) couple water planning models (CALSIM II), physical models (HEC-RAS, DSM2, DSM2-PTM, USBR river temperature model, etc.) and Chinook salmon life cycle models to predict how various salmon populations will respond to suites of management actions, including changes to flow and export regimes, modification of water extraction facilities, and large-scale habitat restoration. In this document, we describe a winter-run Chinook salmon life cycle model (WRLCM). In the following sections, we provide the general model structure, the transition equations that define the movement and survival throughout the life cycle, the life cycle model inputs that are calculated by external models for capacity and smolt survival, and the steps to calibrate the WRLCM.

Winter-run Life Cycle Model (WRLCM)

The WRLCM is structured spatially to include several habitats for each of the life history stages of spawning, rearing, smoltification (physiological and behavioral process of preparing for seaward migration as a smolt), outmigration, and ocean residency. We use discrete geographic regions of Upper River, Lower River, Floodplain, Delta, Bay, and Ocean (Figure 1). The temporal structure of winter-run Chinook is somewhat unique, with spawning occurring in the late spring and summer, the eggs incubating over the summer, emerging in the fall, rearing through the winter and outmigrating in the following spring (Figure 2). We capture these life-history stages within the WRLCM by using developmental stages of eggs, fry, smolts, ocean sub-adults, and mature adults (spawners). The goal of the WRLCM is consistent with that of Hendrix et al. (2014); that is, to quantitatively evaluate how Federal Central Valley Project (CVP) and California State Water Project (SWP) management actions affect Central Valley Chinook salmon populations.

In 2015, the WRLCM was reviewed by the Center for Independent Experts (CIE). In response to recommendations from the CIE, the following modifications were implemented in the WRLCM: 1) divided the River habitat to encompass above Red Bluff Diversion Dam (Upper River) and below Red Bluff Diversion Dam (Lower River); 2) incorporated hatchery fish into the WRLCM; 3) used 95% of observed density as an upper bound for calculation of habitat capacity; 4) re-parameterized the Beverton-Holt function; 5) used appropriate spawner sex-ratios for model calibration to account for bias in Keswick trap capture; 6) modified the WRLCM to a state-space form to incorporate measurement error and process noise; and 7) designed metrics and simulation studies to evaluate model performance. In addition, Hendrix et al. (2014) indicated that future work would use DSM2's enhanced particle tracking model to track salmon survival, which has now been implemented.

Additional comments received in the CIE review that have not been incorporated yet include: 1) expanding spatial structure for spring and fall-run; 2) tracking additional categories of juveniles (e.g., yearling) for applying an LCM to spring-run Chinook; 3) implementing shared capacity for fall and spring-run Chinook; 5) tracking monthly cohorts through the model; and 6) evaluating multiple

model structural forms. We are actively working on improving the WRLCM and developing the spring-run LCM (SRLCM) and fall-run LCM (FRLCM). Many of the CIE recommendations will be implemented with subsequent versions of these models.

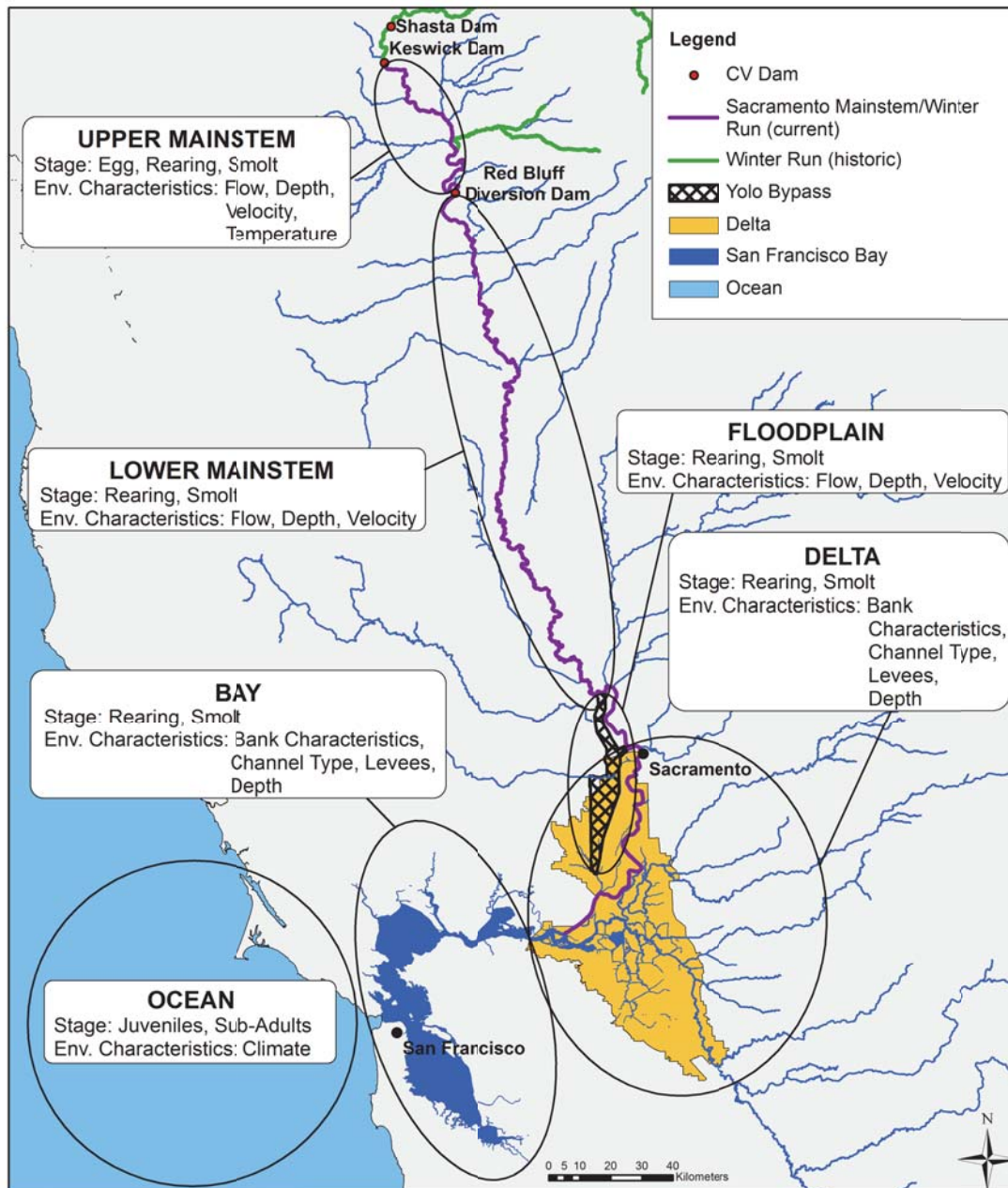


Figure 1. Geographic distribution of Chinook life stages and examples of environmental characteristics that influence survival.

The quantity and quality of rearing and migratory habitat are viewed as key drivers of reproduction, survival, and migration of freshwater life stages. Various life stages have velocity, depth, and temperature preferences and tolerances, and these factors are influenced by water project operations and climate.

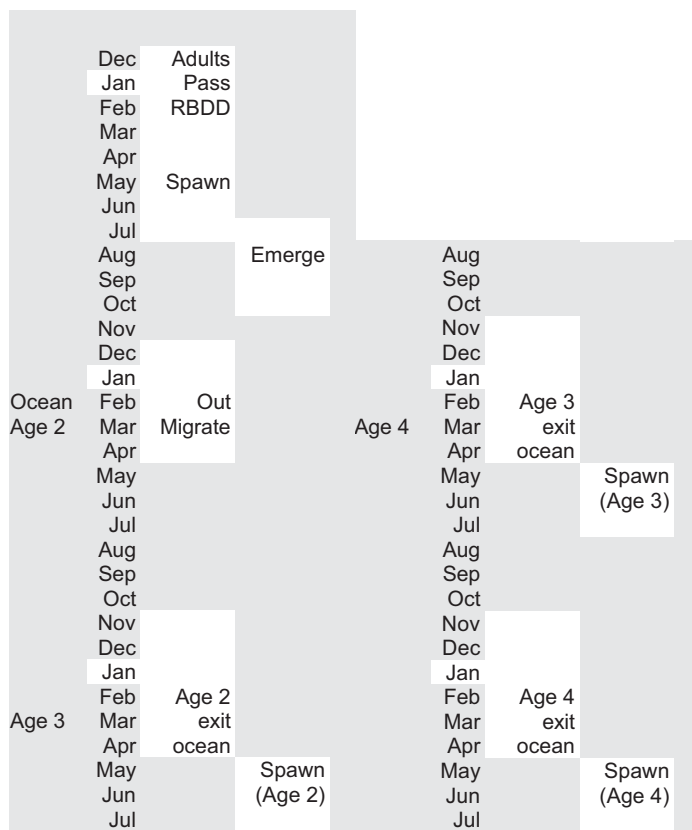
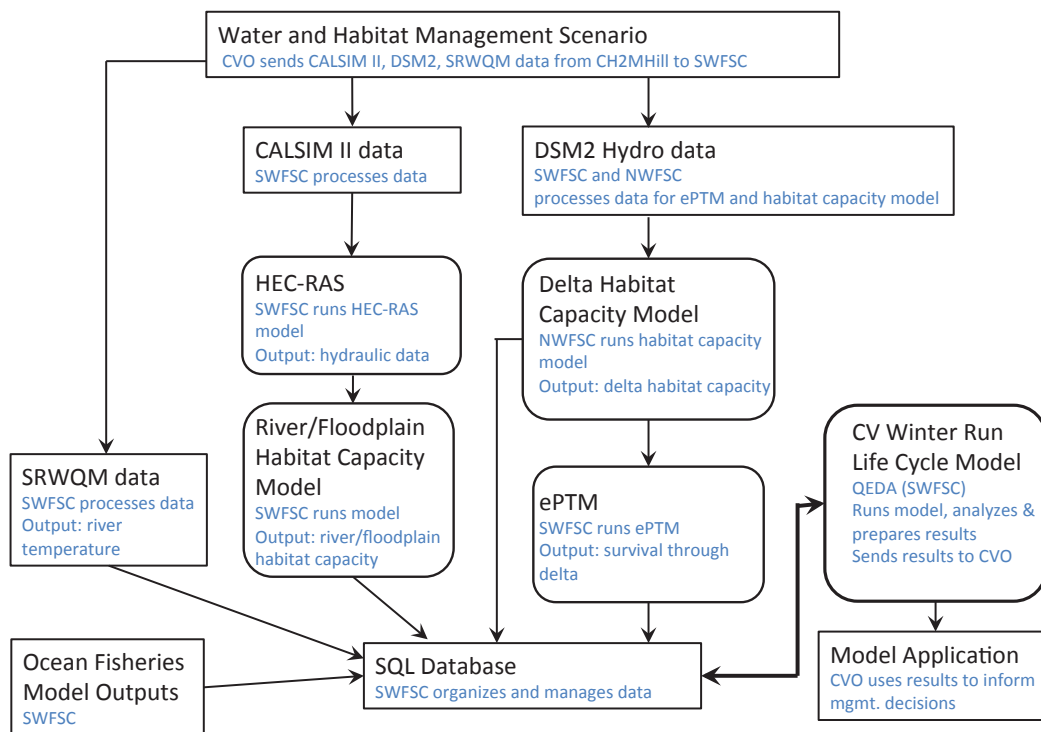


Figure 2. Temporal structure of the winter-run Chinook salmon, each cohort begins in March of the brood year. Figure from Grover et al. (2004).

Hydrology (the amount and timing of flows) is modeled with the California Simulation Model II (CALSIM II). Hydraulics (depth and velocity) and water quality is modeled with the Delta Simulation Model II (DSM2) and its water quality sub-model QUAL, the Hydrologic Engineering Centers River Analysis System (HEC-RAS), the U.S. Bureau of Reclamation’s (USBR) Sacramento River Water Quality Model (SRWQM), and other temperature models. The enhanced particle tracking model (ePTM) makes use of many of these DSM2 related products to calculate survival of outmigrating smolts originating from Lower River, Delta, and Floodplain habitats. Many of the stage transition equations describing the salmon life cycle are directly or indirectly functions of water quality, depth, or velocity, thereby linking management actions to the salmon life cycle. The combination of models and the linkages among them form a framework for analyzing alternative management scenarios (Figure 3).

Central Valley Winter Run LCM Model Linkages



11/29/2016

Figure 3. Submodels that support and provide parameter inputs that feed into the life cycle model.

The life cycle model is a stage-structured, stochastic life cycle model. Stages are defined by development and geography (Figure 1), and each stage transition is assigned a unique number (Figure 4).

II. Model Transition Equations

This section is divided into two parts. In the first part, we explain each of the transitions for the natural origin winter-run Chinook, which are described by the life cycle diagram (Figure 4). In the second part, we explain the transitions for hatchery origin fish. The transitions are described for an annual cohort; however, in most cases we have not included a subscript for the cohort brood year to simplify the equations. For those transitions in which there are multiple cohorts, such as the production of eggs in transition 22, a subscript to distinguish cohort is included in the equation.

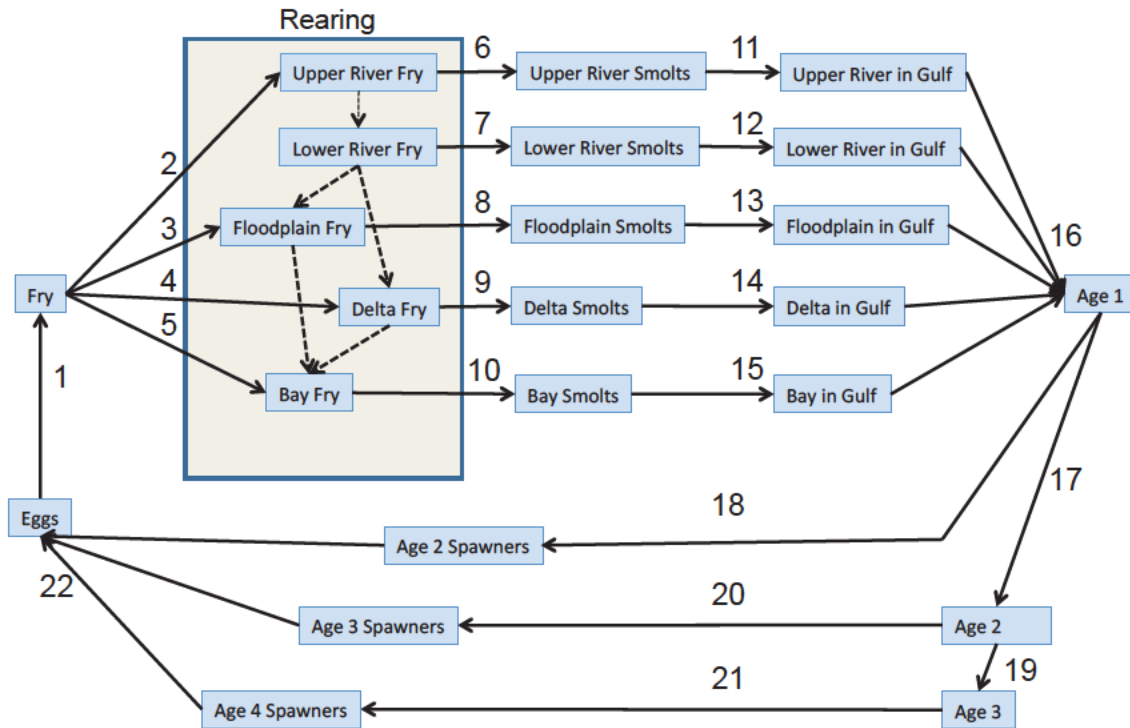


Figure 4. Central Valley Chinook transition stages. Each number represents a transition equation through which we can compute the survival probability of Chinook salmon moving from one life stage in a particular geographic area to another life stage in another geographic area.

Natural Origin Chinook

Transition 1

Definition: Survival from Egg to Fry

$$Fry_{m+2} = Eggs_m * S_{eggs, m}$$

$$\text{logit}(S_{eggs, m}) = \begin{cases} B0_1, & TEMP \leq t.crit \\ B0_1 + B1_1(TEMP_m - t.crit), & TEMP > t.crit \end{cases}$$

where $S_{eggs, m}$ is the survival rate of fry as a function of the coefficients $B0_1$, $B1_1$ and $t.crit$ (model parameter representing the critical temperature at which egg survival begins to decline), the covariate $TEMP_m$ (the average of the month of spawning m and the following 2 months), $\text{logit}(x) = \log(x/[1-x])$ is a function that ensures that the survival rate is within the interval $[0,1]$, for months $m = (2, \dots, 6)$ corresponding to April to August.

Transitions 2 - 5

Definition: Dispersal from fry in the natal reaches as tidal fry to the h habitats = Lower River (LR), Floodplain (FP), Delta (DE), and Bay (BA) in months $m = (5, \dots, 10)$ corresponding to July to December. Remaining fry as rearing fry in the Upper River (UR).

Tidal Fry and Upper River Rearing Fry (Transition 2)

$$TidalFry_m = P_{TF} * Fry_m$$

$$RearFry_{UR,m} = (1 - P_{TF}) * Fry_m$$

where P_{TF} is the proportion of fry moving out of the Upper River as tidal fry, and $RearFry_{UR,m}$ are the number remaining in the Upper River habitat (UR) as rearing fry.

Floodplain Tidal Fry (Transition 3)

Whenever there are flows into the Yolo Bypass, a proportion of the Tidal Fry move into the floodplain habitat:

$$TidalFry_{FP,m} = S_{TF,FP} * TidalFry_m * P_{FP,m}$$

where $P_{FP,m}$ is the proportion of fry that move into the Floodplain habitat, and $S_{TF,FP}$ is the monthly survival of tidal fry in the floodplain. The $P_{FP,m}$ is modeled as a function of the expected flow onto the Floodplain habitat due to proposed modifications of the Fremont Weir.

$$P_{FP,m} = \begin{cases} min.p, & y.flow_m < 100 \\ min.p + \frac{(y.flow_m - 100) * (0.5 - min.p)}{5900}, & 100 \leq y.flow_m \leq 6000 \\ inv.logit\left(\frac{p.rate * (y.flow_m - 6000)}{1000}\right), & y.flow_m > 6000 \end{cases}$$

where $P_{FP,m}$ is the proportion of fry moving into the Floodplain as a function of the coefficients $min.p$ (0.05) and $p.rate$ (1.1), and the covariate $y.flow_m$. The function $inv.logit(x) = e^x / (1 + e^x)$ ensures that the proportion of fry moving into the Floodplain is within the interval [0,1]. The covariate $y.flow_m$ represents the monthly average flow rate (cfs) at the entrance to Yolo Bypass (CALSIM node D160). The relationship between $P_{FP,m}$ and flow is depicted in Figure 5.

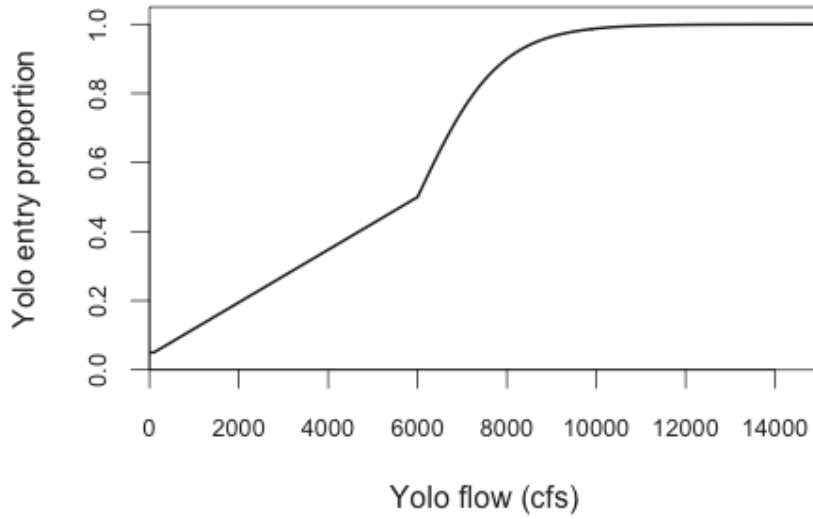


Figure 5. The relationship of Floodplain entry (Yolo bypass) entry proportion (P_{FP}) as a function of Yolo flow.

Delta and Bay Tidal Fry (Transition 4 and 5)

$$TidalFry_{DE,m} = TidalFry_m * (1 - P_{FP,m}) * (1 - P_{TF,BA,m}) * S_{TF,DE,m}$$

$$TidalFry_{BA,m} = TidalFry_m * (1 - P_{FP,m}) * P_{TF,BA,m} * S_{TF,DE,m} * S_{TF,DE-BA}$$

where $S_{TF,DE,m}$ is the survival to the Delta by Tidal Fry.

$$\text{logit}(S_{TF,DE,m}) = B0_4 + B1_4 * DCC_m$$

where $B0_4$ and $B1_4$ are model parameters, and DCC_m is the proportion of the transition month that the DCC gate is open.

$P_{TF,Bay,m}$ is the proportion of fish moving to the Bay from the Delta

$$\text{logit}(P_{TF,Bay,m}) = B0_5 + B1_5 * Q_{RioVista,m}$$

where $B0_5$ and $B1_5$ are model parameters, and $Q_{RioVista,m}$ is the flow anomaly (subtract mean and divide by standard deviation). The mean and standard deviation were calculated from 1970-2014 data at Rio Vista, which was the period of model calibration.

Rearing

Definition: Fry rear among Upper River, Lower River, Floodplain, Delta, and Bay habitats according to a density dependent movement function in months $m = (5, \dots, 10)$ corresponding to July to December.

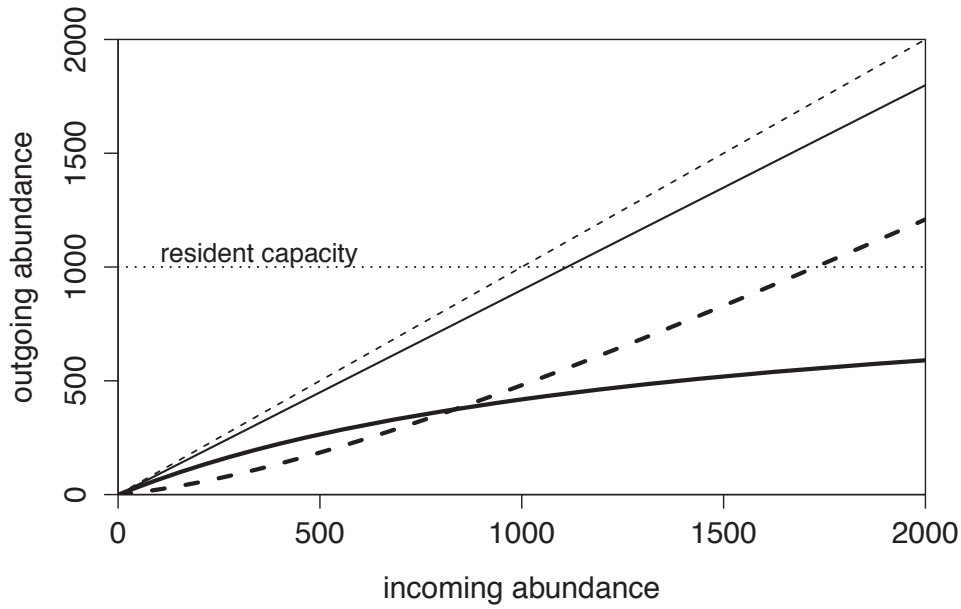


Figure 6. Example of the Beverton-Holt movement function in which the outgoing abundance (thin solid black line) is split between migrants (thick dashed line) and residents (solid dark line), that are affected by the resident capacity (thin dotted line). The 1:1 line (thin dashed line) is also plotted for reference. Parameter values used in the plotted relationship are survival, $S = 0.90$; migration, $m = 0.2$; and capacity, $K = 1000$.

The number of residents in the month is calculated from the following equation (Figure 6):

$$Residents_{h,m} = S_{FRY,h,m} * (1 - mig_{h,m}) * N_{h,m} / (1 + S_{FRY,h,m} * [1 - mig_{h,m}] * N_{h,m} / K_{h,m})$$

$$Migrants_{h,m} = S_{FRY,h,m} * N_{h,m} - Residents_{h,m}$$

where $S_{FRY,h,m}$ is the survival rate in the absence of density dependence, $N_{h,m}$ is the pre-transition abundance composed of *Migrants* from upstream habitats in $m-1$ and *Residents* from the current habitat (Figure 7) in $m-1$, $K_{h,m}$ is the capacity for habitat type h and $mig_{h,m}$ is the migration rate in the absence of density dependence in month m .

The migration rate in the Lower River is modeled as a function of a flow threshold at Wilkins Slough

$$\text{logit}(mig_{LR,m}) = B0_M + B1_M * I(Q_{Wilkins, m} > 400 \text{ m}^3\text{s}^{-1})$$

whereas in all other habitats and months the migration rate $mig_{h,m}$ is a constant value. Survival of resident and migrant fry $S_{FRY,h,m}$ are also constant over habitats and months.

Transitions 6 - 10

Definition: Smolting of *Residents* in the Upper River, Lower River, Floodplain, Delta, and Bay rearing habitats in months $m = (11, \dots, 17)$ corresponding to January to July in the calendar year after spawning.

$$Smolts_{h,m} = P_{SM,m} * Residents_{h,m-1}$$

where $P_{SM,m}$ is the probability of smolting in month m which is assumed to be the same across habitats, by the *Residents* from the previous month ($m-1$) in that habitat.

The probability of smolting is modeled as a proportion ordered logistic regression model of the form:

$$\text{logit}(P_{SM,m}) = Z_k$$

where $-\infty < Z_1 < Z_2 \dots < Z_k < \infty$ are the monthly rates of smoltification based on photoperiod ($k = 1, \dots, 7$ encompassing January to July).

The model performs the following steps during the months in which smoltification occurs:

1. Smoltification of Resident fry
2. Survival and movement of the Migrant fry from the upstream habitats and remaining Resident fry after removing smolts from step 1

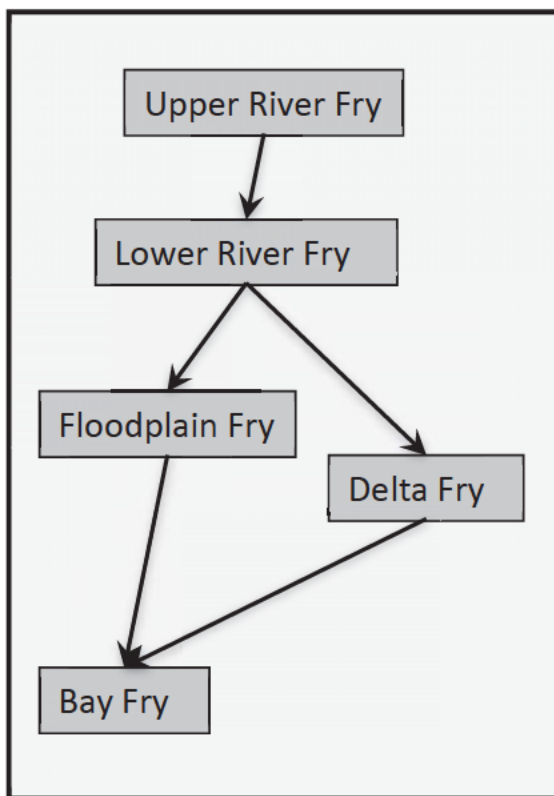


Figure 7. Connectivity among habitats for winter-run Chinook fry. Connections between the Lower River and Floodplain occur due to flooding of the Yolo bypass and are thus ephemeral.

Transitions 11 & 12

Definition: Smolts that reared in the Upper River and Lower River habitats migrate to the Gulf of the Farallones in months $m = (12, \dots, 18)$ corresponding to February to August.

Upper River smolt outmigration (Transition 11)

$$Gulf_{UR,m} = S_{11,UR,m} * S_{G1} * Smolts_{UR,m-1} * \exp(\varepsilon_y)$$

Lower River smolt outmigration (Transition 12)

$$Gulf_{LR,m} = S_{12,LR,m} * S_{G1} * Smolts_{LR,m-1} * \exp(\varepsilon_y)$$

where survival $S_{T,h,m}$ is the smolt survival rate from transition T (11, ..., 15) in habitat h (UR, LR, FP, DE, BA) in month m . The rates $S_{11,UR,m}$ and $S_{12,LR,m}$ are composed of three components: A) survival rate from the Upper or Lower River to the Sacramento River near Sacramento; B) survival through the Delta to Chipps Island; and C) survival from Chipps Island to Golden Gate. The survival rate S_{G1} is the survival rate of smolts originating from the Upper River, Lower River, and Floodplain habitats during ocean entry at the Gulf of Farallones. Finally, the transition to the ocean from all habitats includes a random effect term ε_y that is specific to each year y and is distributed as a normal random variable, that is $\varepsilon_y \sim N(0, \sigma_{\varepsilon}^2)$.

$$S_{11,UR,m} = A_{S_{11,UR,m}} * B_{S_{12,LR,m}} * C_{S_{11}}$$

$$S_{12,LR,m} = A_{S_{12,LR,m}} * B_{S_{12,LR,m}} * C_{S_{11}}$$

The first smolt survival component is modeled as a function of flow at Bend Bridge

$$\text{logit}(A_{S_{11,UR,m}}) = B_{011,UR} + B_{111} * q.bb_m$$

$$\text{logit}(A_{S_{12,LR,m}}) = B_{012,LR} + B_{111} * q.bb_m$$

where $B_{011,UR}$, $B_{012,LR}$ and B_{111} are model parameters, and $q.bb_m$ is monthly flow at Bend Bridge which is the closest station to the Red Bluff Diversion Dam standardized relative to historic Bend Bridge flows from 1970-2014.

$$B_{S_{12,LR,m}} = ptm_{LR,m}$$

where $ptm_{LR,m}$ is a mean monthly survival rate for smolts originating from the Sacramento River through the Delta to Chipps Island as calculated by the enhanced Particle Tracking Model (ePTM, described below). The value $C_{S_{11}}$ is a model parameter representing survival from Chipps Island to Golden Gate and is applicable to smolts originating from all habitats.

Transition 13

Definition: Smolts that reared in the Floodplain migrate to the Gulf of the Farallones in months $m = (12, \dots, 18)$ corresponding to February to August.

$$Gulf_{FP,m} = S_{13,FP,m} * S_{G1} * Smolts_{FP,m-1} * \exp(\varepsilon_y)$$

The rate $S_{13,FP,m}$ is composed of three components: A) survival rate from the Floodplain to the Delta; B) survival through the Delta to Chipps Island; and C) survival from Chipps Island to Golden Gate.

$$S_{13,FP,m} = {}^A S_{13,FP,m} * {}^B S_{13,FP,m} * {}^C S_{11}$$

where ${}^A S_{13,FP,m}$ is survival to insertion into the Floodplain nodes in the ePTM and

$${}^B S_{13,FP,m} = ptm_{FP,m}$$

where $ptm_{FP,m}$ is a mean monthly survival rate for smolts originating from the Floodplain through the Delta to Chipps Island as calculated by the ePTM.

Transition 14

Definition: Smolts that reared in the Delta migrate to the Gulf of the Farallones in months $m = (12, \dots, 18)$ corresponding to February to August.

$$Gulf_{DE,m} = S_{14,DE,m} * S_{G2} * Smolts_{DE,m-1}$$

The rate $S_{13,DE,m}$ is composed of two components: A) survival through the Delta to Chipps Island; and B) survival from Chipps Island to Golden Gate. The survival rate S_{G2} is the survival rate of smolts in the nearshore from Delta and Bay habitats during ocean entry at the Gulf of Farallones.

$$S_{G2} = \text{logit}(\text{inv.logit}(S_{G1}) + D_{G2})$$

$$S_{14,DE,m} = {}^A S_{14,FP,m} * {}^C S_{11}$$

where ${}^A S_{14,FP,m} = ptm_{DE,m}$

Transition 15

Definition: Smolts that reared in the Bay migrate to the Gulf of the Farallones with an associated migration survival in months $m = (12, \dots, 18)$ corresponding to February to August.

$$Gulf_{BA,m} = S_{15,BA} S_{G2} Smolts_{BA,m-1}$$

where $S_{15,BA}$ is the survival from the Bay habitat to the Golden Gate.

Transition 16

The total number of Age 1 from all habitats arriving in a given month can be calculated by summing across each of the individual rearing areas. Furthermore, earlier arriving fish are retained in the Age 1 stage and an ocean survival rate is applied to those fish that were already in the Age 1 stage in the previous month. Fish arrive into the Age 1 stage in months $m = (12, \dots, 21)$ corresponding to February through October.

$$Age1_m = Age1_{UR,m} + Age1_{LR,m} + Age1_{FP,m} + Age1_{DE,m} + Age1_{BA,m} + Age1_{m-1} * S_{17}^{1/4}$$

Transition 17

Definition: Survival in the ocean from Age 1 to Age 2 (for Chinook that remain in the ocean)

$$Age2 = Age1_{m=21} * (1 - M_2) * S_{17}$$

where S_{17} is a model parameter representing the survival rate of Age 1 fish in the ocean to Age 2 and M_2 is a model parameter representing the maturation rate that leads to 2 year old spawners. The model transitions from a monthly time step (used for months 1 through 20) to an annual time step (used for Age 2, Age 3 and Age 4 fish) in this transition, thus the S_{17} survival represents a 4-month survival rate from 21 months to 24 months.

Transition 18

Definition: Maturation and migration for Age 2 males and females that will spawn as 2 year olds

$$Sp_{2,F} = Age1_{m=21} * S_{17} * M_2 * Fem_{Age2} * S_{sp2}$$

$$Sp_{2,M} = Age1_{m=21} * S_{17} * M_2 * (1 - Fem_{Age2}) * S_{sp2}$$

where S_{17} and M_2 are model parameters for maturation and survival as described in Transition 17. Fem_{Age2} is a model parameter representing the proportion of Age 2 spawners that are female, and S_{sp2} is a model parameter representing the natural survival rate of Age 2 spawners from the ocean to the spawning grounds.

Transition 19

Definition: Survival in the ocean from Age 2 to Age 3 (for Chinook that remain in the ocean)

$$Age3 = Age2 * (1 - I_3) * S_{19} * (1 - M_3)$$

where I_3 is the fishery impact rate for Age 3 fish, S_{19} is a model parameter representing natural survival rate for fish between Age 2 and Age 3, and M_3 is a model parameter representing maturation rate of Age 3 fish.

Transition 20

Definition: Maturation and migration for Age 3 males and females that will spawn as 3 year olds

$$Sp_{3,F} = Age2 * (1 - I_3) * S_{19} * M_3 * Fem_{Age3} * S_{sp3}$$

$$Sp_{3,M} = Age2 * (1 - I_3) * S_{19} * M_3 * (1 - Fem_{Age3}) * S_{sp3}$$

where I_3 is the Age 3 fishery impact rate, and M_3 and S_{19} are the Age 3 maturation and survival rates as described in Transition 19. Fem_{Age3} is a model parameter representing the proportion of Age 3 and 4 spawners that are female, and S_{sp3} is a model parameter representing the natural survival rate of Age 3 spawners from the ocean to the spawning grounds.

Transition 21

Definition: Maturation and migration for Age 3 males and females that will spawn as 4 year olds

$$Sp_{4,F} = Age3 * (1 - I_4) * S_{21} * Fem_{Age3} * S_{sp4}$$
$$Sp_{4,M} = Age3 * (1 - I_4) * S_{21} * (1 - Fem_{Age3}) * S_{sp4}$$

where I_4 is the Age 4 fishery impact rate, S_{21} is a model parameter representing survival rate from Age 3 to Age 4, Fem_{Age3} is a model parameter representing the proportion of Age 3 and 4 spawners that are female, and S_{sp4} is a model parameter representing the natural survival rate of Age 4 spawners from the ocean to the spawning grounds.

Transition 22

Definition: Number of eggs produced by spawners of Ages 2 – 4 in months $m = (2, \dots, 6)$ corresponding to April to August.

$$Eggs_m = \frac{\sum_{j=2}^4 TSp_{j,F} * P_{SP,m} * V_{eggs,j}}{1 + \frac{\sum_{j=2}^4 P_{SP,m} * TSp_{j,F} * V_{eggs,j}}{K_{Sp,m}}}$$

where TSp_j are the total number of female spawners of age $j = 2, 3, 4$ (composed of both natural and hatchery origin), $V_{eggs,j}$ is the number of eggs per spawner of age $j = 2, 3, 4$, $K_{Sp,m}$ is the capacity of eggs in the spawning grounds per month, and $P_{SP,m}$ is the proportion of spawning that occurs in month m and is a function of April average temperature at Keswick Dam. Because the April temperature can vary among years, the monthly distribution varies as well to reflect observed patterns in spawn timing among the years from 1999 to 2012. Please see Appendix A for description of the analysis of historical patterns in spawn timing.

$$TSp_{2,F} = Sp_{2,F} + Sp_{2,F,Hatchery}$$

$$TSp_{3,F} = Sp_{3,F} + Sp_{3,F,Hatchery} - hat.f$$

$$TSp_{4,F} = Sp_{4,F} + Sp_{4,F,Hatchery}$$

$$hat.f = 0.15 * Sp_3 \quad (\text{min} = 10; \text{max} = 60)$$

where $hat.f$ is the number of spawning females removed for use as hatchery broodstock, and $Sp_{j,Hatchery}$ for $j = (2,3,4)$ is the spawners of age j hatchery origin, which are described below in the *Hatchery Origin Chinook* section.

Hatchery Origin Chinook

Transition 1H

Definition: Survival of hatchery fish from eggs to Age 2

$$Age2_{Hatchery} = hat.f * 3000 * H_{S1}$$

$$H_{S1} = 2.3 * Age2_{Natural} / Fry_{Natural}$$

where H_{S1} is the hatchery-origin survival rate from pre-smolt at release to Age 2 in the ocean, $Age2_{Natural}$ is the number of natural-origin Chinook that survived to Age 2 and remained in the ocean, and $Fry_{Natural}$ is the number of natural origin emerging Fry (see Transition 1 for Natural Origin Chinook). The multiplier of 3000 hatchery smolts per spawner was obtained from Winship et al. (2014). The multiplier of 2.3 was used to equate hatchery origin survival to the end of age 2 to natural origin survival to the end of age 2 as described in Winship et al. (2014).

Transition 2H

Definition: Maturation and spawning for hatchery origin Age 2

$$Sp_{2,F,Hatchery} = Age2_{Hatchery} * M_2 * Fem_{Age2} * S_{sp2}$$

$$Sp_{2,M,Hatchery} = Age2_{Hatchery} * M_2 * (1 - Fem_{Age2}) * S_{sp2}$$

where the coefficients are described under Transition 18.

Transition 3H

Definition: Survival of hatchery origin fish in the ocean from Age 2 to Age 3 (for Chinook that remain in the ocean)

$$Age3_{Hatchery} = Age2_{Hatchery} * (1 - I_3) * S_{19} * (1 - M_3)$$

where the coefficients are described under Transition 19.

Transition 4H

Definition: Maturation and spawning for hatchery origin Age 3

$$Sp_{3,F,Hatchery} = Age2_{Hatchery} * (1 - I_3) * S_{19} * M_3 * Fem_{Age3} * S_{sp3}$$

$$Sp_{3,M,Hatchery} = Age2_{Hatchery} * (1 - I_3) * S_{19} * M_3 * (1 - Fem_{Age3}) * S_{sp3}$$

where the coefficients are described under Transition 20.

Transition 5H

Definition: Survival and maturation rate for hatchery origin Age 4

$$Sp_{4,F,Hatchery} = Age3_{Hatchery} * (1 - I_4) * S_{21} * Fem_{Age3} * S_{sp4}$$

$$Sp_{4,M,Hatchery} = Age3_{Hatchery} * (1 - I_4) * S_{21} * (1 - Fem_{Age3}) * S_{sp4}$$

where the coefficients are described under Transition 21.

Fishery Dynamics

To simulate the winter-run population dynamics under alternative hydrologic scenarios, we include fishery dynamics that are consistent with the current fishery control rule (NMFS 2012) (Figure 8). For each year of the simulation, the impact rate for age 3 (I_3) was calculated from the control rule by

obtaining the 3-year trailing geometric average of spawner abundance. The age-4 impact rate (I_4) in that year was calculated as double the instantaneous age-3 impact rate (Winship et al. 2014).

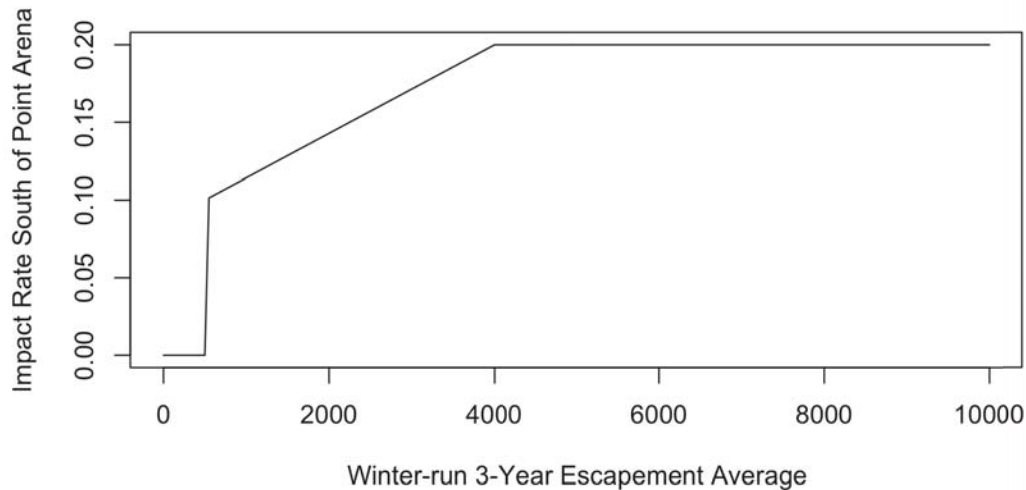


Figure 8. Fishery control rule determining the level of Age 3 impact rate as a function of trailing 3-year geometric mean in winter-run escapement.

III. Inputs to the Winter-run life-cycle model

Water Temperature

The life cycle model (LCM) incorporates monthly average temperature below Keswick Dam into the definition of egg to fry survival. The water temperature can be obtained from water quality gages on the Sacramento River (for model calibration) or from a forecasted water temperature model, such as the as the Sacramento River Water Quality Model (SRWQM).

Fisheries

Estimates of impact rates on vulnerable age classes of Chinook salmon are computed as part of the Pacific Fisheries Management Council (PFMC) annual forecast of harvest rates and review of previous years' observed catch rates. For runs that are not actively targeted, such as winter-run and spring-run Chinook, analyses of coded wire tag (CWT) groups are used to infer impact rates for these races (e.g., O'Farrell et al. 2012).

Habitat Capacity

Juvenile salmonids rear in the mainstem Sacramento River, delta, floodplain, and bay habitats (Figure 1). The model incorporates the dynamics of rearing by using density-dependent movement out of habitats as a function of capacity for juvenile Chinook. The capacities of each of the habitats are calculated in each month using a series of habitat-specific models that relate habitat quality to a spatial capacity estimate for rearing juvenile Chinook salmon. Habitat quality is defined uniquely for

each habitat type (mainstem, delta, etc.) with the goal of reflecting the unique habitat attributes in that specific habitat type. For example, the mainstem habitat quality is a function of velocity and depth (Liermann et al. 2005). Higher quality habitats are capable of supporting higher densities of rearing Chinook salmon, with the range of densities being determined from studies in the Central Valley and in river systems in the Pacific Northwest where appropriate.

Defining habitat capacity. For each habitat type (mainstem, delta, and bay), capacity was calculated each month as:

$$K_i = \sum_{j=1}^n A_j d_j$$

where K_i is the capacity for a given habitat type i , n is the total number of categories describing habitat variation, A_j is the total habitat area for a particular category, and d_j is the maximum density attributable to a habitat of a specific category. Three variables were determined for each habitat, the ranges of each were divided into high and low quality, and all combinations were examined, resulting in a total of eight categories ($2 \times 2 \times 2$) of habitat quality for each habitat type (Table 1). The exception was mainstem habitats (Upper River and Lower River), which were subdivided into 4 (2×2) bins of habitat quality. Ranges of high and low habitat quality were based on published studies of habitat use by Chinook salmon fry across their range and examination of data collected by USFWS within the Sacramento-San Joaquin Delta and San Francisco Bay.

Defining maximum densities. Determining maximum densities for each combination of habitat variables is complicated by the fact that most river systems in the Central Valley are now hatchery-dominated with fish primed for outmigration. In addition, the Central Valley river system is at historically low natural abundance levels compared to expected or potential density levels. Because of this deficiency in the Central Valley system, salmon fry density data from the Skagit River system were used, which in contrast has very low hatchery inputs, has been monitored in mainstem, delta, and bay habitats, and exhibits evidence of reaching maximum density in years of high abundance (Greene et al. 2005; Beamer et al. 2005). These data from the Skagit River were compared with Central Valley density estimates calculated by USFWS. For each of these data sets, the upper 90 to 95 percentile levels of density defined a range of maximum density levels, assuming that the highest five percentile of density levels were sampling outliers. The comparison indicated that Skagit River values represented conservative estimates of maximum density (Figure 9).

Table 1. Habitat variables influencing capacity for each habitat type.

| Habitat type | Variable | Habitat quality | Variable range |
|--------------|----------------|-----------------|--|
| Mainstem | Velocity | High | ≤ 0.15 m/s |
| | | Low | > 0.15 m/s |
| Delta | Depth | High | > 0.2 m, ≤ 1 m |
| | | Low | ≤ 0.2 m, > 1 m |
| | Channel type | High | Blind channels |
| | | Low | Mainstem, distributaries, open water |
| Bay | Depth | High | > 0.2 m, ≤ 1.5 m |
| | | Low | ≤ 0.2 m, > 1.5 m |
| | Cover | High | Vegetated |
| | | Low | Not vegetated |
| Bay | Shoreline type | High | Beaches, marshes, vegetated banks, tidal flats |
| | | Low | Riprap, structures, rocky shores, exposed habitats |
| | Depth | High | > 0.2 m, ≤ 1.5 m |
| | | Low | ≤ 0.2 m, > 1.5 m |
| Salinity | High | ≤ 10 ppt | |
| | Low | > 10 ppt | |

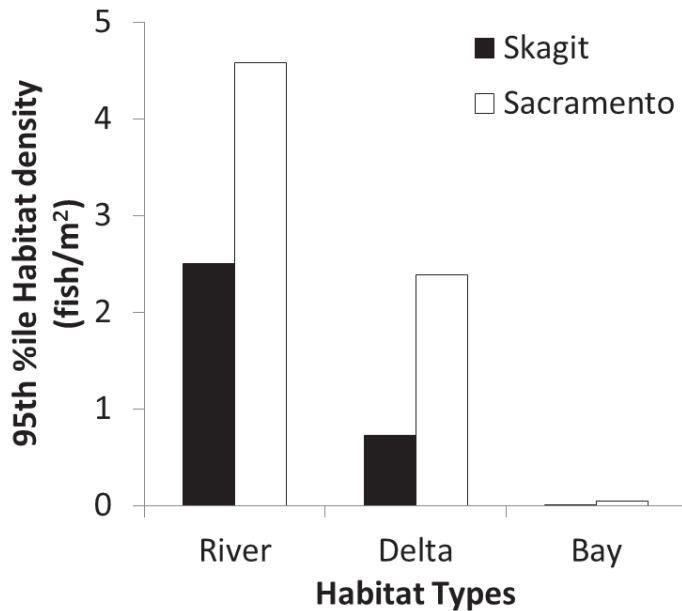


Figure 9. 95th percentile values of densities in river, delta, and bay habitats in the Skagit and Sacramento Rivers. Skagit data are based on electroshocking in mainstems and beach seining in delta and bay habitats (Beamer et al. 2005), while Sacramento data are based on beach seining across all habitat types (USFWS, 2005).

Determining habitat areas. Two approaches were used to map the spatial extents of different combinations of habitat variables. In the mainstem and floodplain, the HEC-RAS model divides the river into units based on multiple cross-sections defining depth ranges (Figure 10). Each unit defined by the cross-sections has velocity parameters associated with it. Different levels of flow in a given

month or year change the distribution of velocity and depth. Total habitat area in each of the eight classes is calculated by integrating over the river channels modeled by HEC-RAS.

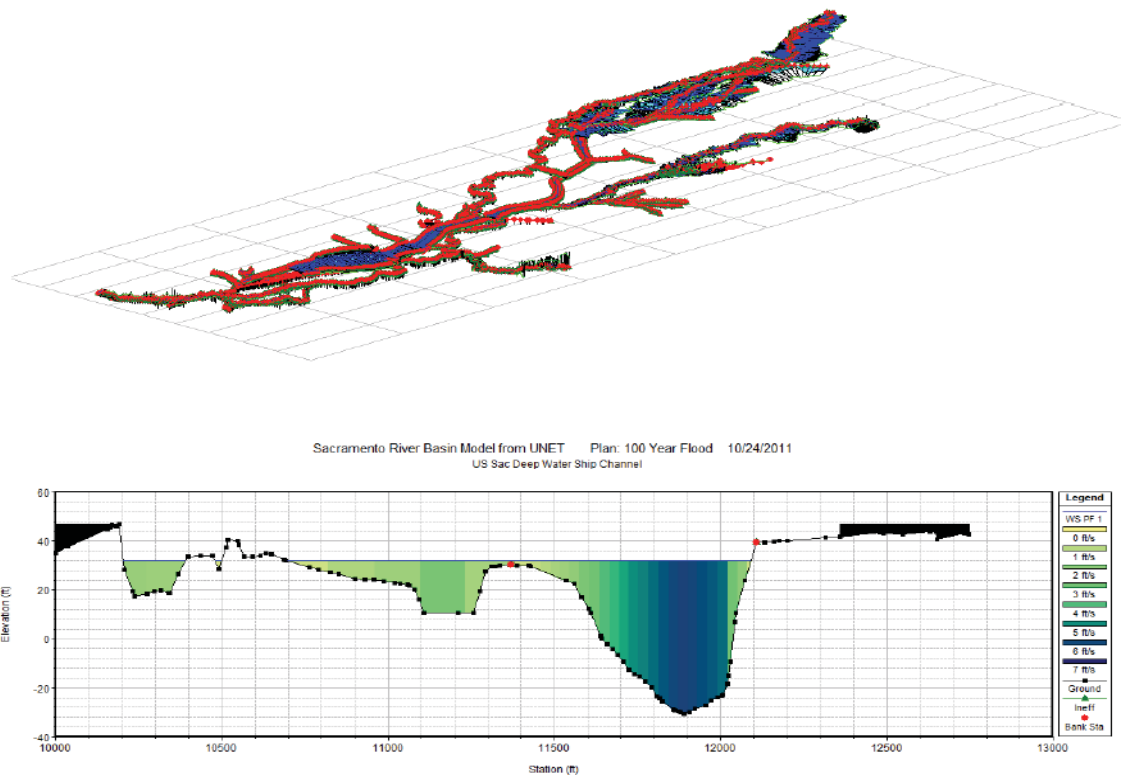


Figure 10. HEC-RAS model cross sections of the Sacramento River mainstem and floodplain (upper panel), and a visualization of a single cross-section, showing depth and velocity differences (lower panel).

For the delta and bay, channel type, depth, cover, salinity, and shoreline type were mapped from existing delta and bay Geographic Information Systems (GIS) products (Figure 11). Delta and bay polygons¹ were classified into high quality habitat types (blind tidal channels) and low quality habitat types (mainstem, distributaries, large water bodies, and bay). For the channel typing, several datasets comprised the base GIS layers, including National Wetlands Inventory (NWI) wetland polygons, San Francisco Estuary Institute’s Bay Area Aquatic Resource Inventory’s (BAARI) stream lines and polygons, Hydro24ca channel polygons (USBR 2006, Mid-Pacific Region GIS Service Center), aerial photos and Google Earth. The Hydro24ca channel data included channel types such as major river, slough, lake and several other types. When channel type could not be defined for a given reach, aerial photos and attributes from surrounding channels were used to estimate channel type. National Wetland Inventory (NWI) GIS data served as base channel and wetland data. NWI data provides comprehensive data coverage as well as detailed wetland categories that were required. However, NWI data did not have enough information to distinguish accessibility for juveniles. Thus, Bay Area Aquatic Resource Inventory (BAARI) data were used as a reference to identify accessible

¹ A closed shape used in GIS mapping that is defined by a connected sequence of x, y coordinate pairs, where the first and last coordinate pair are the same and all other pairs are unique.

wetlands from NWI polygons. For the areas that BAARI data did not cover, levee GIS layers were overlain to estimate accessible wetland habitat.

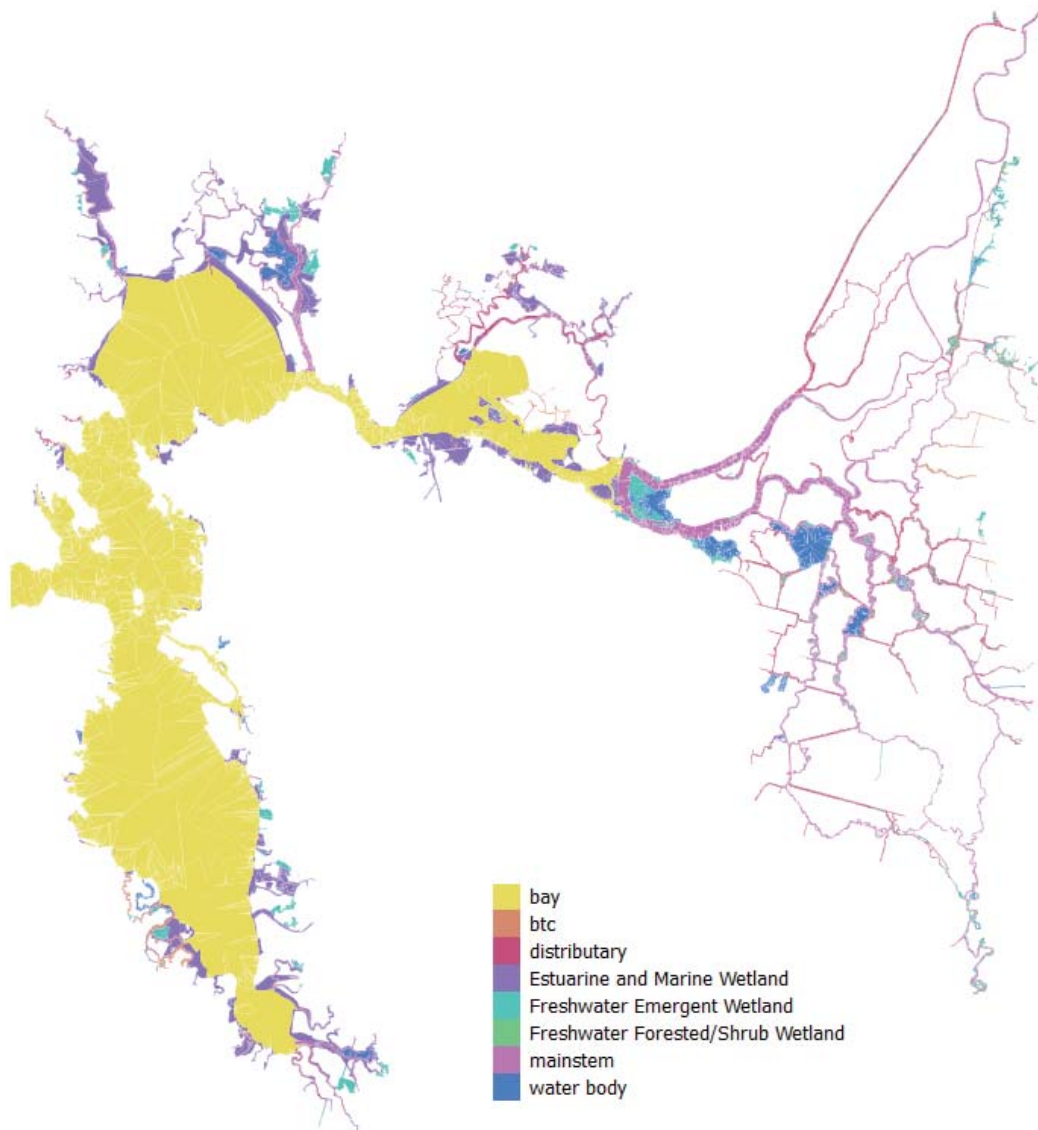


Figure 11. Habitat types delineated for the Sacramento Delta and San Francisco Bay. The abbreviation “btc” stands for blind tidal channel.

Most channel types could be mapped using these datasets except for the blind tidal channels. Instead of directly mapping blind tidal channels, we estimated these areas using allometric relationships between wetland areas and blind tidal channel areas. We tested allometric equations developed in the Skagit River by Beamer et al. (2005) and Hood (2007) to determine which equations were best suited to apply to the Central Valley and chose an allometric equation that returned conservative estimation results:

$$\text{BTC (ha)} = 0.0024 * \text{Wetland(ha)}^{1.56}$$

We also applied the minimum area requirement (0.94 ha) to form blind tidal channels in a wetland from Hood (2007).

Salinity is another factor influencing habitat availability for juvenile Chinook salmon that can vary with water flow. The X2 position describes the distance from Golden Gate Bridge to the 2 ppt isohaline position near the Sacramento Delta (Jassby et al. 1995). This distance predicts amount of suitable habitat for various fish and other organisms. Based on observations of high likelihood of fry presence in water with salinity of up to 10 ppt in both Skagit River and San Francisco Bay fish monitoring data, we defined the low-salinity zone for Chinook as salinity < 10 ppt (i.e., habitats upstream of X10). We calculated X10 values as 75 percent of X2 values (Monismith et al. 2002, Jassby et al. 1995), and mapped these across San Francisco Bay.

Another axis used to evaluate habitat is vegetated cover along river banks. Areas associated with cover were assumed to be higher quality habitats because they provide protection from predators (Semmens 2008) and offer subsidies of terrestrial insect prey. Such habitats are preferred in other systems by Chinook salmon (Beamer et al. 2005, Semmens 2008). The extent of these areas was estimated using Coastal Change Analysis Program (C-CAP) Land Use/Land Cover (LULC) layers. We defined sheltered habitat as forested or shrub covered areas and assumed that other areas, such as urban and bare land, did not provide sheltered habitat.

Restricting habitat areas based on connectivity. Our first analysis of habitat areas assumed all regions of the Delta were equally accessible to Chinook salmon fry. This assumption may be incorrect, however, because much of the fish monitoring has shown that fry do not inhabit certain areas in the Delta. Therefore, a spatial connectivity mask, or exclusion zone, was developed to exclude certain areas from the habitat mapping. This exclusion zone was produced using month- and year-specific fish monitoring data (Figure 12). Poisson regression models were used to predict fish counts based on the relationships between fish counts in beach seine datasets and several covariates including river system (Sacramento or San Joaquin), distance of sampling site to its mainstem (m), physical channel depth (m), physical channel width (m), and DSM2 water stage (m). We selected these parameters based on Akaike's Information Criterion (AIC) analysis of the Poisson regression models with various combinations of the parameters. The resulting Poisson model equation was used to produce a presence-absence map for the entire delta (Figure 12). Restricted capacity estimates were generated by summing habitat areas with predicted fry presence.

Modeling capacity for preferred and no action alternatives. The geospatial tools described above were used to make predictions of capacities of preferred and no action alternatives by routing Calsim2 runs of alternatives through HEC-RAS and DSM2 models. Model changes for these runs included the lowering of the diversion for the Yolo Bypass in HEC-RAS for both alternatives and the diversions and underground tunnels in DSM2 for the preferred alternative.

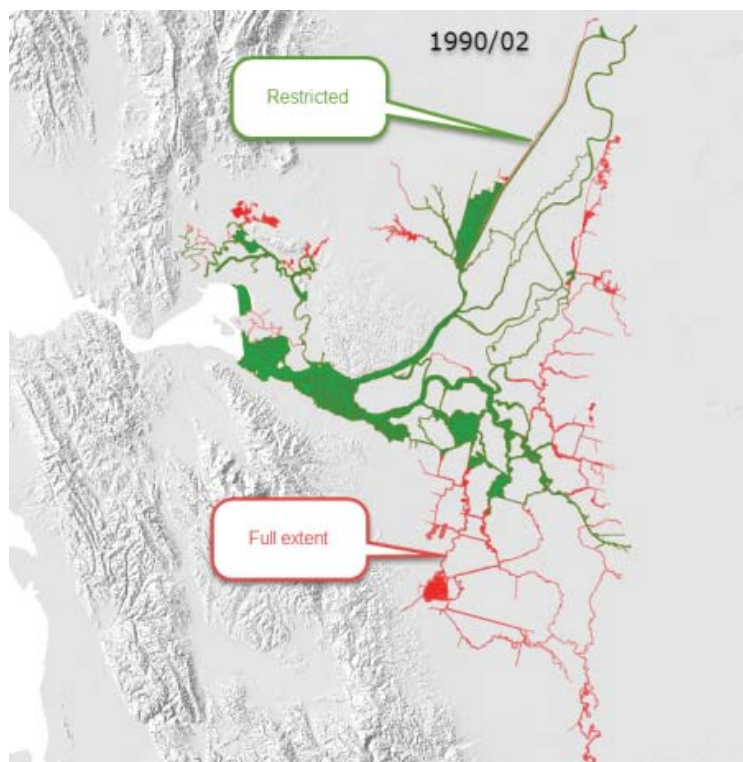


Figure 12. Example results of reduced connectivity applied to the February (02) 1990 map. The presence/absence prediction for connected habitat areas is designated as “Restricted” (green), a smaller area than the full extent of the Sacramento Delta (red).

Enhanced Particle Tracking Model

The survival rate of juvenile Chinook salmon within and migrating through the Delta is modeled using the Enhanced Particle Tracking Model (ePTM). This rate is defined as the survival at Chippis Island of simulated juvenile salmon (SJS) released at any location within the Delta. The ePTM survival computation includes swimming behavior and predation mortality (Sridharan et al., in prep.). The ePTM is based on the Delta Simulation Model II Particle Tracking Model (DSM2 PTM) developed by the Department of Water Resources (DWR), California.

DSM2

The DSM2 PTM transports particles on a one-dimensional network representation of the Delta, driven by the flows computed by HYDRO, the hydrodynamic module of DSM2 written in FORTRAN (Anderson and Mierzwa, 2002). The DSM2 HYDRO module computes the flow and stage at different locations in the Delta by solving the cross-sectionally averaged one-dimensional shallow water wave equations on a network of links, continuously stirred tank reactors (CSTR) and nodes which respectively represent channels, flooded and leveed islands, floodplains and forebays, and channel junctions (Figure 13). River inflows and in-delta consumptive use flows are estimated from DAYFLOW, an estimated account of net flows in and out of the Delta. Gate operations are provided by DWR. Details of the numerical solution method can be found in DeLong et al. (1997). DSM2 HYDRO is typically run with a timestep of 15 minutes to one hour.

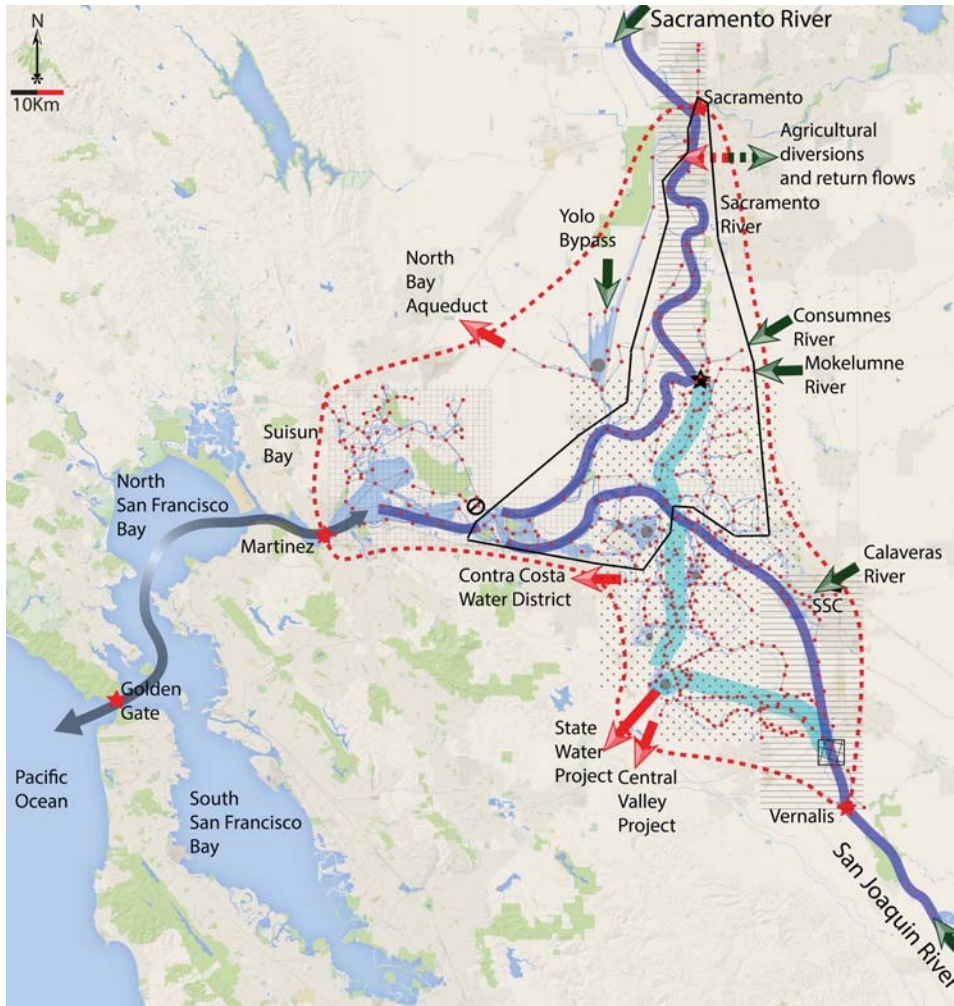


Figure 13. Sacramento-San Joaquin Delta and DSM2 grid. Dashed red line represents boundary of the Delta. Green arrows represent inflows, red arrows represent outflows, grey arrow represents tidal flow. Grey lines, grey circles and red dots respectively represent DSM2 links, reservoirs and nodes. Dark blue lines represent the mainstem Sacramento and San Joaquin Rivers. Light blue lines represent the canals and Old and Middle River Corridors. The black star represents the Delta Cross Channel, the black circle represents the salinity control gate in Montezuma Slough. The black cross-hatched box represents the temporary barriers. The riverine, transitional and tidal ePTM behavioral reaches are represented respectively by the horizontal, dotted, and checkered hatching. The DSM2 nodes at which SJS are released to represent river, floodplain and Delta smolt and fry are represented respectively by the red star at Sacramento, the black circle at the Southern tip of the Yolo Bypass floodplain, and all the nodes within the black border.

The DSM2 PTM module, written in JAVA, is a pseudo three-dimensional model with a turbulent law of the wall logarithmic vertical velocity (Prandtl, 1935) and a fourth order polynomial transverse velocity profile (Wilbur, 2000) imposed onto the solved mean flows through a cross-section. The links are represented as rectangular prismoids whose cross-sections preserve the hydraulic radii and water column depth in the channels they represent. It uses constant cross-sectional eddy diffusivities in a zeroth-order turbulence closure to move particles laterally and vertically. Particles are advected in the streamwise direction with the hydrodynamic velocity at their locations and moved randomly in the lateral and vertical direction with the diffusivities at their locations using Forward Euler numerical integration. DSM2 PTM is capable of modeling about 5,000 particles (Kimmerer and Nobriga, 2008). It does not have any temporal interpolation of hydrodynamic

quantities between DSM2 HYDRO timesteps, and randomizes particles arriving at nodes and assigns them to new links based on the flow splits at the nodes. Their new cross-sectional positions are also randomized. The ePTM builds on the basic framework of the DSM2 PTM.

ePTM

The ePTM adds juvenile salmon swimming behavior and predation mortality to the DSM2 PTM (Jackson et al., in prep.). Apart from these additions, the ePTM linearly interpolates all hydraulic and hydrodynamic quantities between DSM2 HYDRO timesteps to account for SJS movement within an ePTM time substep. Broadly, the scope of the ePTM can be summarized into its representation of the hydrodynamics, the fish behavior, and the mortality of SJS.

Hydrodynamics

SJS trajectories are given by the Weiner process (Visser, 1997)

$$\frac{dx}{dt} = u + u_s; \frac{dy}{dt} = R_y \sqrt{\frac{2 \varepsilon_H}{r \Delta t}}; \frac{dz}{dt} = R_z \sqrt{\frac{2 \varepsilon_V z}{r \Delta t}}$$

where u is the hydrodynamic velocity at the particle position, u_s is the swimming velocity, ε_H and ε_V are the lateral and vertical eddy diffusivities, Δt is the ePTM timestep, R_Y and R_Z are uniform random variables between -1 and 1, r is the variance of a uniform distribution and is equal to 1/3.

The velocities and diffusivities in ePTM are given by

$$u = U f_V f_H$$

$$f_V = \begin{cases} 1 + \frac{\sqrt{C_D}}{\kappa} \left[1 + \ln \left(\frac{z}{H} \right) \right] & ; z > z_0; z_0 = 0.03m; C_D \approx 0.03 \\ 0 & ; z \leq z_0 \end{cases}$$

$$f_H = 1.2 + 0.3 \left(\frac{2y-W}{W} \right)^2 - 1.5 \left(\frac{2y-W}{W} \right)^4$$

where U is the mean velocity of flow, the linearization of the friction force has been performed with the bottom drag coefficient C_D (e.g., Wang et al., 2009), and the bed shear stress has been parameterized using a constant bottom roughness height z_0 (e.g. Kundu and Cohen, 2002).

and

$$\varepsilon_H = 0.6 H u_*; \varepsilon_V = 0.067 H u_*; u_* = \sqrt{C_D} U$$

where H is the depth of the water column and u_* is the friction velocity.

Time substeps are chosen as the time step required to limit particle displacement at any given timestep to within 10 percent of the smallest dimension of the channel. A particle leaves a given channel through its upstream or downstream end when its streamwise displacement during a timestep exceeds the distance between its current position and the end of the channel. The channel bottom, banks and free surface are treated as fully reflecting boundaries.

Currently, SJS are not allowed to enter reservoirs or flooded islands because the DSM2 PTM does not have a module for dealing with reservoirs. Also, the routing of SJS through junctions follows the randomization based on the flow splits of the DSM2 PTM. The next update of ePTM will include a CSTR model for flooded islands, as well as a parameterization of SJS movement at channel junctions based on fitting beta distributions to observed juvenile salmon distributions at key junctions in the Delta (Perry and Pope, p.c.).

Behavior

The ePTM incorporates behavior by adding a biological swimming velocity to the flow velocity at the location of the SJS. The SJS also hold position via Selective Tidal-Stream Transport (STST) (Gibson, 2003), a hypothesis for optimal energy expenditure while achieving average travel speeds greater than the average flow velocity in tidal regions. During the ebb phase of the tide, the SJS allow themselves to be advected. On a flood tide, when the upstream flow exceeds some threshold, they hold position (Liao, 2007). The ePTM also parameterizes diel swimming behavior (Chapman et al., 2013) by assigning a probability of swimming during the light hours. Lastly, ePTM includes phenomenological parameters of oceanward direction assessment, and confusion of SJS due to confounding flows such as exports due to pumping (Table 2).

Table 2. Behavior and habitat parameters in the ePTM.

| Parameter | Value in riverine reach | Value in transition reach | Value in tidal reach |
|---|--|--|--|
| Swimming speed (m/s) | 0.015±0.31 | 0.23±0.83 | 0.25±1.91 |
| Threshold oceanward directed velocity above which fish hold position (m/s) | 0.28 | 0.05 | 0.41 |
| Probability of swimming during the day | 0.15 | 0.31 | 0.28 |
| Probability of being confused about direction of flow | $0.5 - 0.25 \left(\frac{\bar{Q}}{Q_{RMS}} - 3.99 \right)$ | $0.5 - 0.25 \left(\frac{\bar{Q}}{Q_{RMS}} - 4.62 \right)$ | $0.5 - 0.25 \left(\frac{\bar{Q}}{Q_{RMS}} - 2.91 \right)$ |
| Probability of assessing direction of flow at a given time step | 0.01 | 0.01 | 0.01 |
| Mean free path length between predator encounters (Km) | 395 | 151.4 | 329.8 |
| Random predator encounter speed which includes tidal fluctuations as well (m/s) | 0.048 | 0.048 | 0.048 |

Rationale behind the choice of behavior parameters

As the advection due to the river flow decreases from the riverine to transition reaches, SJS have to rely greater on their swimming velocity to migrate than the river advection, and hence swimming speed increases.

The rationale behind the choice of mean free path length between predator encounters is that more time spent in a particular region is likely to increase the chance of predation within that region. This is elaborated subsequently. In the riverine reaches, the channels are long (~10Km) and there are very few multi-channel junctions. Therefore, SJS trajectories looped over many junctions (i.e., when a fish moves downstream and then back upstream again via the same or different channels during different phases of the tide) are unlikely, and the path length between predator encounters is very large. In the transition reach, the many channel junctions and very small channel lengths (~100-500m) are likely to induce an increased number of predator encounters due to looped SJS trajectories, and so the path length between predator encounters is small here. In the tidal reach, there are fewer channel junctions and longer channels (~1Km) but with greater likelihood of looped SJS trajectories than in the riverine reaches, and so the path length between predator encounters is larger than in the transition reach but smaller than in the riverine reaches.

The biological parameters of random predator-prey encounter speed and the probability of assessing the downstream direction are theoretically independent of the nature of the flow. We treat these variables as constant across all reaches in the ePTM. In reality, the random predator-prey encounter speed is likely to be spatially heterogeneous due to different interactions between predators and prey in different conditions (Anderson, p.c.). The probability of assessing the downstream direction is set to 0.01. This ensures that the recurrence interval of the assessment, which is the inverse of the probability of assessment, is approximately 24 hours. In other words, SJS are likely to assess the oceanward direction once every two tidal cycles. While there is little support for such a recurring assessment of the correct migration direction by juvenile salmon in literature, a diel assessment of flow conditions would at least allow for the filtering of the principle tidal constituents up to the longest periods that contribute to flow reversal in the San Francisco Bay-Delta system, i.e. K1, O1 and S1.

Chapman et al. (2013) observed that approximately 75-90% of tracked juveniles migrated during the dark hours in the Sacramento River, while about 60-70% migrated during the dark hours in the Delta and Suisun Bay. These values are qualitatively reflected in the probability of swimming during the day.

In the confusion parameterization, the probability of improper orientation is a logistic function of the signal-to-noise ratio (SNR) that saturates at a probability of 0.5 for low SNRs (simulated juveniles can only randomly assess the downstream direction) and at a probability of 0 for high SNRs (simulated juveniles can always assess the downstream direction accurately). The shape of the logistic function is defined by two parameters: the location of the half-saturation point, and the steepness of the logistic function. A slope of the logistic function of -0.25 captures the range of SNRs commonly observed in the Delta within the linear portion of the curve and the half-saturation point is higher in the riverine and transition reaches than the tidal reaches, reflecting larger likelihood of confusion with distance away from the ocean. The half-saturation point increases in the transition reach compared to the riverine reaches as the influence of the tides becomes strong compared to the mean river flow.

Predation Mortality

The ePTM adds predator-induced mortality according to the XT model (Anderson et al., 2005). The probability of a SJS surviving passage through a reach, S , is as follows:

$$S = e^{-\left(\frac{1}{\lambda}\sqrt{x^2 + \omega^2 t^2}\right)}$$

where x is the distance traveled and t is the travel time. The mean free path, λ , is

$$\lambda = \frac{1}{\rho\pi r^2}$$

where ρ is the density of predators and r is the encounter distance. The term ω is the random component of prey speed. The implementation of the XT model in the ePTM involves recording the x and t for each channel that a SJS traverses in a given 15-minute time step. A survival probability for each of these sub time steps is then calculated using the λ values for the individual channels. The overall probability that the SJS survives the 15-minute time step is the product of the survival probabilities of the sub time steps, i.e.:

$$S = \prod_{i=1}^n e^{-\left(\frac{1}{\lambda_i}\sqrt{x_i^2 + \omega_i^2 t_i^2}\right)}$$

where n is the number of channels that the SJS traversed during the time step, x_i is the distance traveled in channel i , t_i is the time spent in channel i , and λ_i and ω_i are the channel-specific mortality parameters. In the ePTM, only the parameters λ_i and ω_i are specified explicitly (Table 2).

$$\begin{aligned} \frac{\bar{Q}}{Q_{\text{RMS}}} &\geq 1; && \text{Riverine} \\ 0.1 \leq \frac{\bar{Q}}{Q_{\text{RMS}}} &< 1; && \text{Transitional} \\ \frac{\bar{Q}}{Q_{\text{RMS}}} &< 0.1; && \text{Tidal} \end{aligned}$$

where T_T is the duration of a tidal cycle, and $Q_{\text{RMS}} = \sqrt{\frac{1}{T_T} \int_0^{T_T} Q^2 dt - \bar{Q}^2}$.

ePTM application

A minimum of 10000 SJS released from any location on the DSM2 grid is required to achieve statistically repeatable results. These releases are performed uniformly over a period of one month, which is the timestep size in the LCM. However, releasing 10000 simulated juveniles is computationally expensive. As a tradeoff between statistical repeatability and performance, for riverine and tidal salmon fry and smolt survival, 1000 SJS are released uniformly each month at Sacramento, and in the floodplain node (Figure 13). The survival probability of each SJS escaping the Delta at Chipps Island is resampled with replacement to produce 1000 survival probabilities, whose mean and standard deviation give a measure of the expected value of the survival and its variance. A similar exercise is carried out for Delta fry and smolt, with 100 particles released uniformly over all the nodes within the North and Central Delta corridor (Figure 13). In this case, a release of 100

particles per node is sufficient, as this results in more than 15,000 SJS released over the total number of release nodes. The net Delta survival is computed as

$$S_D = \frac{\sum_i^n N_i S_i}{\sum_i^n N_i}$$

where n is the number of resampled outcomes, or 1000, N_i is the number of times the i^{th} SJS arriving at Chipps Island is resampled, and S_i is the survival of the i^{th} SJS. Such a resampling procedure ensures that the net Delta survival is an average of contributions from all the nodes of the Delta weighted by the escapement from each node. It is to be noted that the definition of the Delta as shown in Figure 1 represents the likely passage of late-fall and winter-run Chinook salmon smolts. This can be readily modified to include other nodes in the Delta. The number of simulated salmon resampled from each release node are weighted by the relative maximum supported population at each node with respect to the total maximum supported population in the whole Delta by

$$N_m = \frac{\sum_{j=1}^8 k_j A_j}{\sum_{i=1}^m (\sum_{j=1}^8 k_j A_j)} \times n$$

where N_m is the number of particles contributing to the resampling from the release node m , A_j is area and k_j is the carrying capacity of the j^{th} type of habitat class associated with that node, in which habitat class is characterized into 8 classes by the velocity and depth of the flow, channel bottom roughness, type of shoreline, vegetation cover, salinity intrusion (X2), carrying capacity and available area (Hendrix et al., 2014).

There are certain months during which habitat information may be unavailable. In these cases, a lookup table was developed in MATLAB to interpolate survivals from ePTM results for those months. The lookup table was based on the ratio of export flow to inflow, ratio of the RMS tidal flow to the mean river flow through Carquinez Strait, ratio of time the Delta Cross Channel was open to the total duration of one month, and ratio of flow through the Delta Cross Channel to the flow in the Sacramento River. There is no correlation assumed between these parameters. Each parameter is assumed to have equal weight. The lookup table operation is performed by first choosing the year-month combination which minimizes the 4-dimensional Euclidean distance between the hydrology of the year-month, r , that does not have the habitat information,

$$M_{\text{LOOKUP}} = \min_{v_i} \left\{ \sqrt{\left[\left(\frac{Q_E}{Q_I} \right)_i - \left(\frac{Q_E}{Q_I} \right)_r \right]^2 + \left[\left(\frac{Q_{\text{RMS}}}{\bar{Q}} \right)_i - \left(\frac{Q_{\text{RMS}}}{\bar{Q}} \right)_r \right]^2 + \left[\left(\frac{T_{\text{DXC OPEN}}}{T} \right)_i - \left(\frac{T_{\text{DXC OPEN}}}{T} \right)_r \right]^2 + \left[\left(\frac{Q_{\text{DXC}}}{Q_{\text{SAC}}} \right)_i - \left(\frac{Q_{\text{DXC}}}{Q_{\text{SAC}}} \right)_r \right]^2} \right\}$$

Then, the habitat factor for MLOOKUP is computed as

$$S = \frac{N_{r,\text{CHIPPS}}}{N_r} \times \frac{N_{\text{LOOKUP}}}{N_{\text{LOOKUP,CHIPPS}}} \times \frac{\overline{S_{\text{LOOKUP}}}}{\overline{S_{\text{LOOKUP,RESAMPLED}}}} \times S_{\text{LOOKUP}}$$

where N_{LOOKUP} and N_r are the number of particles released in the lookup year-month and in month r respectively, $N_{\text{LOOKUP,CHIPPS}}$ and $N_{r,\text{CHIPPS}}$ are the number of particles escaping the Delta in the lookup year-month and in month r , respectively, $\overline{S_{\text{LOOKUP}}}$ is the mean survival before resampling, and $\overline{S_{\text{LOOKUP,RESAMPLED}}}$ is the mean survival after resampling, and S_{LOOKUP} is an actual survival in the

lookup year-month, where the factor $\frac{S_{\text{LOOKUP}}}{S_{\text{LOOKUP,RESAMPLED}}}$ is included to correct for sampling bias from different nodes.

Alternative Scenario Applications

Currently, the ePTM can represent four scenarios: (i) the current geomorphology and hydrology of the Delta (Current), (ii) a historic representation of the Delta before Liberty Island flooded (Historic), (iii) operational scenarios due to the California Water Fix, in which canals are in place to divert freshwater from the Sacramento River upstream of the Delta Cross Channel to a forebay, but water is not pumped through these canals (No Action Alternative, NAA), and (iv) these diversion canals are actively withdrawing water, (Preferred Alternative, PA). These scenarios are represented as alternate DSM2 grids, which can be applied individually in the ePTM (BDCP, 2013; Figure 14).

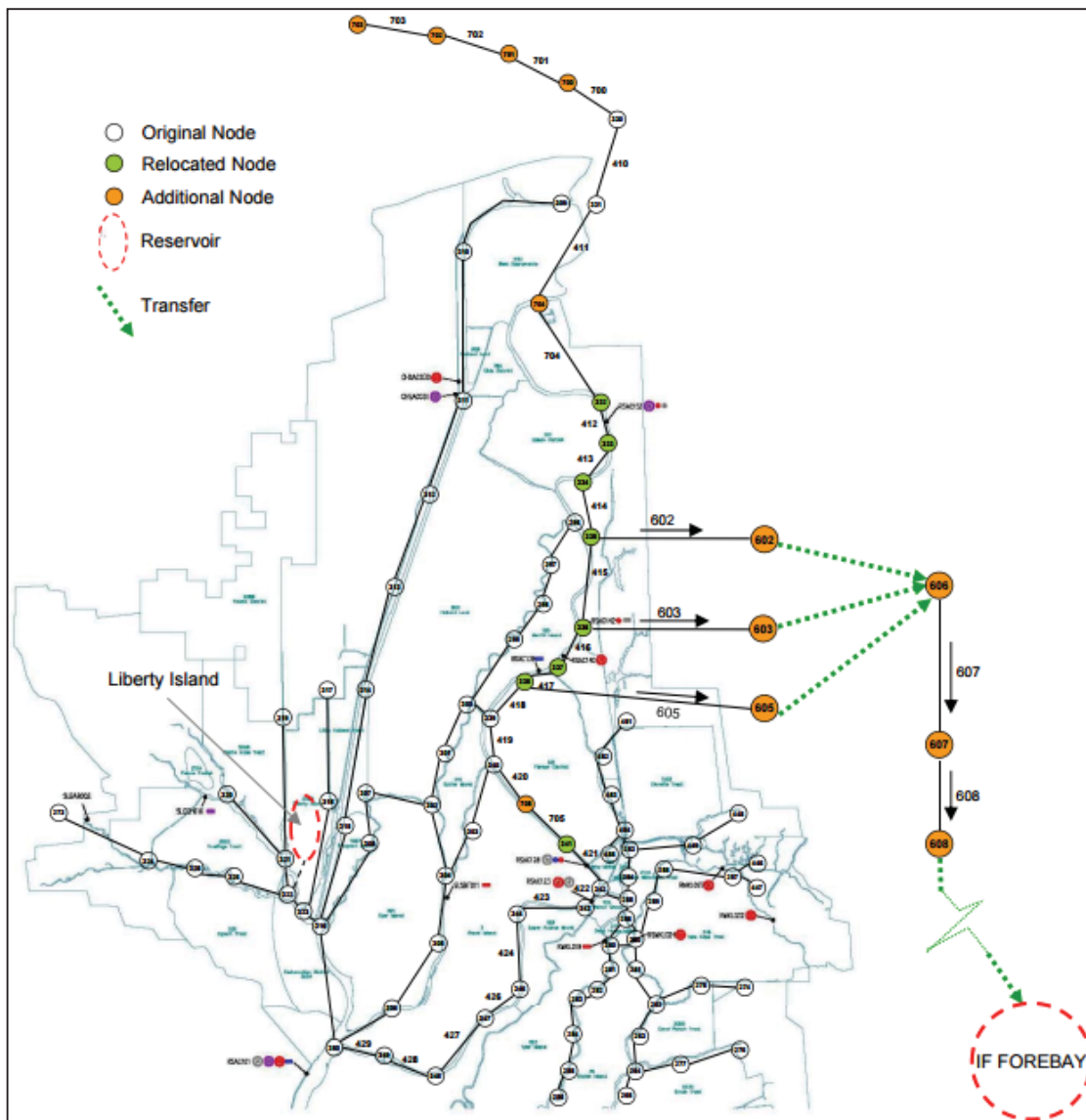


Figure 14. Changes to the DSM2 grid for the NAA and PA scenarios (BDCP, 2013).

The potential implications of the NAA scenario is that while active diversion of freshwater does not occur, the presence of screens may impact habitat quality near the diversion canals. These locations may also become predation hotspots. The habitat quality and area associated with this alternative can be modified accordingly.

The potential implications of the PA scenario is that when active diversion of freshwater occurs, a number of salmon fry and smolt may become entrained in this flow, and abrade against the screens, thereby reducing their survivability significantly. The locations of the intakes may also become predator hotspots. Finally, the reduced freshwater flow may reduce the quality of the habitat, and intensify the effect of predation, and migratory confusion. The ePTM accounts for water diversion automatically by intensifying the effect of confounding pumping and tidal flows, thereby increasing the confusion of SJS. Their routing through channel junctions is also adversely affected by the reduced flows. Reduced survivability due to screen abrasion could be incorporated by reducing the weight of each release in the Sacramento River location, so that the final river fry and smolt survival can be modified as

$$S = \alpha S_0$$

where S_0 is the original survival, S is the modified survival, and α represents the fraction of fish unaffected by abrasion with the screens. Further, reduced survival can also be incorporated by randomly assigning reduced swimming velocity and increased probability of confusion to some SJSs released in the Sacramento River location. The effect of predation hotspots can be incorporated by reducing the mean free path length between predator encounters, and increasing the predator encounter speed in the links near the diversion canals.

Caveats

The ePTM results are based on a simplified one-dimensional network representation of the Delta, and hence do not account for complex geo-morphological and hydrodynamic transport and mixing phenomena such as tide induced chaotic dispersion, wind generated transport and gravitational circulation. The ePTM results do not include the effects of environmental stressors such as water quality, temperature, nutrients, channel scale, temporal variability in predation dynamics, and foraging behavior or energy management dynamics. There is a significant data gap in addressing more complex spatio-temporal patterns in biological behavior and habitat interactions, as well as a need for easy model deployment and speed, so the ePTM parameterizes only simple hypothesis about these effects.

IV. Model Calibration

The WRLCM framework is flexible in that it may be used to generate many different trajectories of abundance and spatial patterns of habitat use by varying the parameters of the model. The WRLCM should reflect historical trends and spatial patterns in abundance, however. As a result, we calibrated the WRLCM to multiple winter-run abundance indices by fixing some model parameters and estimating other parameters with a statistical fitting algorithm.

One goal of the WRLCM was to construct a model that was sensitive to alternative hydromanagement actions in the Central Valley; thus the model was structured such that it is sensitive to hydrologic drivers. An unintended consequence of this approach is that the statistical properties of the model are not optimal. In particular, some model parameters are not uniquely identifiable; that is, the same abundance can occur through several different parameter combinations. Because this property of the LCM makes statistical estimation difficult, the values of some parameters must be constrained using biological information, previous studies, or expert opinion, so that other parameters can be estimated. We provide the parameters that were constrained and provide justification for their values before moving to the statistical estimation of the remaining parameters.

Fixed parameters and their justifications

Spawn timing parameters

Historically, the spawning of winter-run Chinook has not been uniform among the months April to August. Instead, higher proportions of winter-run spawned in June and July relative to April, May, and August. In addition, the proportions of winter-run that spawned in each month were not constant across years, but instead varied yearly. We analyzed the historical proportion spawning among each month from 2003 – 2014 using carcass counts (assuming a 2 week period between spawning and senescence), and estimated the proportion of winter-run spawning in each month as a function of April temperatures at Keswick (Appendix A). We compared this model to one that used a static proportion among years, and found that the model based on April temperatures outperformed the static model. The general relationship identified through this multinomial regression model was that hotter April temperatures caused later initiation of spawning in winter-run Chinook. This may be explained mechanistically if the female spawners were laying their eggs to target an emergence time. Hotter temperatures in April indicated that a shorter incubation window was needed, whereas cooler temperatures indicated a longer incubation window. Please see Appendix A for additional information on this analysis.

These equations provided a method of shifting spawning distribution among months as a function of April temperatures (Table 3 and Appendix A). The April water temperatures were standardized in the analysis and thus need to be standardized for use in the simulation model.

Table 3. Fixed parameter values related to monthly spawn timing.

| Parameter | Value | Description |
|------------|---------|---|
| BO_{Apr} | -4.145 | Intercept for proportion of spawners in April |
| $B1_{Apr}$ | 0.0538 | Effect of temperature on proportion of spawners in April |
| BO_{May} | -1.796 | Intercept for proportion of spawners in May |
| $B1_{May}$ | -0.2031 | Effect of temperature on proportion of spawners in May |
| BO_{Jul} | -0.332 | Intercept for proportion of spawners in July |
| $B1_{Jul}$ | 0.3852 | Effect of temperature on proportion of spawners in July |
| BO_{Aug} | -3.443 | Intercept for proportion of spawners in August |
| $B1_{Aug}$ | 0.7921 | Effect of temperature on proportion of spawners in August |

Tidal fry related parameters

Winter-run Chinook generally have not had a high tidal fry proportion (on the order of less than 5%). Furthermore, the location of tidal fry has varied among years, and they have been susceptible to movement downstream in the Sacramento River under high flow conditions (Pat Brandes, USFWS *personal communication*). The WRLCM parameters for the fry stage reflected these assumptions (Table 4).

Table 4. Fixed parameter values related to the tidal fry stage.

| Parameter | Value | Description |
|-------------|-------|---|
| $P_{TF,m}$ | 0.047 | Proportion tidal fry |
| $S_{TF,FP}$ | 0.731 | Survival tidal fry in floodplain |
| $P_{FP,m}$ | 0.881 | Proportion tidal fry to Floodplain if flooding |
| BO_4 | 0.5 | Average survival tidal fry to delta intercept |
| $B1_4$ | -1.0 | Effect of DCC gate (value is in logit space)* |
| BO_5 | 0.5 | Average proportion of tidal fry to bay intercept |
| $B1_5$ | 2.0 | Effect of Rio Vista flow (value is in logit space)* |

*Values in logit space are the untransformed values used in the logit function of the transition equation

Smoltification timing parameters

The timing of smoltification of winter-run Chinook salmon historically begins in January with a majority of winter-run sized smolts outmigrating by March (delRosario et al. 2013). In the WRLCM, all fry are assumed to have smolted by April and migrating in May (Table 5). The timing of smoltification in the WRLCM has been parameterized to coincide with winter-run sized Chinook salmon in Chipps Island trawl data (delRosario et al. 2013) and by using Chipps Island abundance indices as described below in the *Parameter Estimation* section.

Table 5. Smoltification timing parameters for winter-run Chinook.

| Parameter | Value | Description |
|-----------|-------|----------------------------|
| Z_1 | 0.269 | January smolt probability |
| Z_2 | 0.5 | February smolt probability |
| Z_3 | 0.953 | March smolt probability |
| Z_4 | 1 | April smolt probability |
| Z_5 | 1 | May smolt probability |
| Z_6 | 1 | June smolt probability |
| Z_7 | 1 | July smolt probability |

Maturation rate probabilities

The age-specific maturation probabilities for winter-run Chinook salmon were fixed to values based on analysis of coded wire tagged hatchery fish (Grover et al. 2004). The probability of maturation of age 2 fish was 0.10 (M_2), the conditional probability of maturation at age 3 was 0.90 (M_3), and the conditional probability of maturation at age 4 was 1.0.

Age-specific sex ratios were applied to obtain age and sex specific escapement values. Males dominate age-2 escapement, thus the female sex ratio for age-2 fish (Fem_{Age2}) was set at 0.01. Estimates of the proportion of age-3 female spawners (Fem_{Age3}) may vary among years, and we accounted for this historical annual variability by using an annual sex spawner ratio value calculated from Keswick trap counts 2001 – 2014 (mean = 0.595, sd = 0.077). These values were also used in the annual calculation of natural origin escapement from carcass surveys over the period 2001 – 2014 (Doug Killam, CDFW Redding, CA, *personal communication*). In the absence of an estimate of the age-3 sex ratio, a value of 0.5 was assumed for 1970 – 2000.

Egg production per age-2 female ($V_{eggs,2}$) was 3200 for age 2 females (Newman and Lindley, 2006) and production per age-3 and age-4 female ($V_{eggs,3}$ and $V_{eggs,4}$) was 5000 (Winship et al. 2014).

Smolt survival

The ePTM calculates month and year-specific smolt survival probabilities; however, some survival probabilities were needed to move the smolts from their areas of rearing to the location in which

the ePTM survival rates were applied. Smolt survival from the Lower River to the Delta ($BO_{11,LR}$) was fixed at 0.8 (estimates of survival ranged from 0.73 - 0.875 Colusa to Sacramento in the 2012-2015 WR acoustic tag data, Arnold Ammann, SWFSC NMFS Santa Cruz *personal communication*). Smolt survival from the Upper River to the Delta ($BO_{10,UR}$) was fixed at 0.4 (estimates of survival averaged 0.456 from release to Sacramento in the 2012-2015 WR acoustic tag data, Arnold Ammann, SWFSC NMFS Santa Cruz *personal communication*). Smolt survival from the Yolo bypass to insertion into the DSM2 grid for incorporation into the ePTM ($AS_{13,FP}$) was assumed to be 0.924 per month.

Survival of smolts from Chipps Island to the Golden Gate bridge (cS_{11}) was assumed to be 0.82, and survival of smolts that reared in the Bay to the Golden Gate bridge ($S_{15,BA}$) was assumed to be 0.5.

Ocean survival

Survival of smolts that reared in the Upper River, Lower River, and Yolo habitats (S_{G1}) have the same gulf survival, which is estimated (see below in the *Parameter Estimation* section). The survival of smolts from the Delta and Bay habitats (S_{G2}) had survivals that were reduced slightly from those of the River and Yolo habitats to reflect lower quality rearing conditions affecting ocean entry survival (i.e., $D_{G2} = -0.5$ in the logit function for survival during entry into the gulf).

Survival during the first four months in the ocean (S_{17}) was assumed to have a rate of 0.79, which equates to an annual survival of 0.5, whereas annual survival in the ocean for age-3 and age-4 (S_{19} and S_{21}) was assumed to be 0.8. These annual natural survival rates are consistent with winter-run reconstruction conducted annually as part of the fishery management of Sacramento River salmon (Grover et al. 2004, O'Farrell et al. 2012). Annual impact rates of age-3 (I_3) and age-4 (I_4) were obtained from estimated harvest rates over the 1970- 2014 period (O'Farrell and Satterthwaite 2015). Survival of age-2 (S_{sp2}), age-3 (S_{sp3}), and age-4 (S_{sp4}) through the freshwater prior to spawning is assumed to be 0.9 to incorporate in-river harvest, which historically included levels of approximately 7 percent (Grover et al. 2004) and pre-spawn mortality.

Formulation of the Floodplain habitat access for calibration

To reflect the historical dynamics of access to the Floodplain habitat (Yolo bypass), the following transition equation was used to describe the proportion of Tidal Fry that enter the floodplain habitat ($P_{FP,m}$)

$$P_{FP,m} = B1_{FP} * I(Q_{Verona,m} > 991.1 \text{ m}^3\text{s}^{-1})$$

where $Q_{Verona,m}$ was the Sacramento River flow at Verona in month m , $I()$ is an indicator function that equates to 1 when the condition in the parenthesis is met, and $B1_{FP}$ is the proportion of fry that enter the Yolo under flooding conditions, which was 0.8.

Statistical estimation

One of our objectives is to ensure that the WRLCM is capable of reflecting the historical patterns in winter-run Chinook population dynamics in the Sacramento River. In order to meet this objective, we calibrated the LCM to observed winter-run indices of abundance throughout the life cycle (Table 6). Not all indices of abundance were available for the entire period of model calibration of 1970-2014. This data limitation is not a problem for fitting the WRLCM, however. The WRLCM can be fit to the specific indices of abundance for the period over which they were available by pairing

observed indices of abundance with WRLCM predictions over the appropriate period. Then, the sampling distribution provided a likelihood function by which the model predictions were statistically evaluated given the observed data (Hilborn and Mangel 1997).

This type of model, in which multiple data sources are used to inform multiple life-history stages, is called an integrated population model and has notable advantages over piece-wise model composition (Newman et al. 2014). In particular, the model parameter estimates can utilize all of the available data simultaneously, which can improve the parameter estimates by allowing the model to “fill in the gaps” over portions of the life cycle that are unobserved (Newman et al. 2014).

Table 6. Indices of abundance used to calibrate the winter-run life cycle model.

| Data | Date | Coefficient of Variation | Sampling Distribution | Data time step |
|---|----------------------|---|------------------------------|-----------------------|
| Natural Escapement | 1970-2014 | 0.15 (1970-1986) 0.5 (1987-2000) 0.15 (2001-2014) | lognormal | Annual |
| RBDD monthly juvenile counts | 1996-1999, 2002-2014 | 0.85 | lognormal | Monthly |
| Knights Landing monthly catches | 1999 - 2008 | NA | multinomial | Monthly |
| Chippis Island monthly juvenile abundance | 2008 - 2011 | 1.5 | lognormal | Monthly |

Maximum Likelihood Estimation

Given the fixed parameter values described above, the remaining parameters were estimated in a statistical fitting framework. An initial evaluation of model complexity (not shown) indicated that approximately 10 parameters were identifiable in the mechanistic portion of the model, depending upon which parameters were chosen. We estimated 8 parameters in addition to 45 annual random effects (i.e, the ϵ_y) in the model calibration.

These parameters were estimated by maximizing the likelihood (the likelihood specified by the sampling distribution) of observing the winter-run abundance indices (Hilborn and Mangel 1997). That is, parameter combinations can be used to make predictions on the escapement in each year, the number of juveniles passing RBDD in each month, the catches at Knights Landing, and monthly abundance estimates at Chippis Island. Some parameter combinations provide predictions that are closer to the observed abundance indices than others. The parameter combination that provides the closest fit to the observed indices is the one that maximizes the likelihood, and is thus called the maximum likelihood estimate (MLE).

Model parameters were estimated using an Expectation-Maximization algorithm (Dempster et al. 1977). The specific implementation of the algorithm optimizes the fit across different dimensions and has also been termed a gradient search method (Neal et al. 1998; Hastie et al. 2011). In short, the algorithm obtains maximum likelihood estimates for different components of the parameters, cycling through the parameter list to maximize the likelihood in a piece-wise fashion. In our case we used two blocks of parameters: 1) parameters associated with the mechanistic population dynamics

and 2) the annual random effects. The calibration used a statistical search algorithm in which lower and upper bounds were specified to maintain parameter values in biologically realistic ranges (optim using the BFGS fitting algorithm with box constraints in the R programming language – RCDT 2016).

Fits to abundance indices

Fits to the abundance indices generally followed patterns in the observed data. Annual patterns in natural origin escapement were well estimated by the model (Figure 15), as were monthly patterns in juvenile abundance estimates at RBDD (Figure 16).

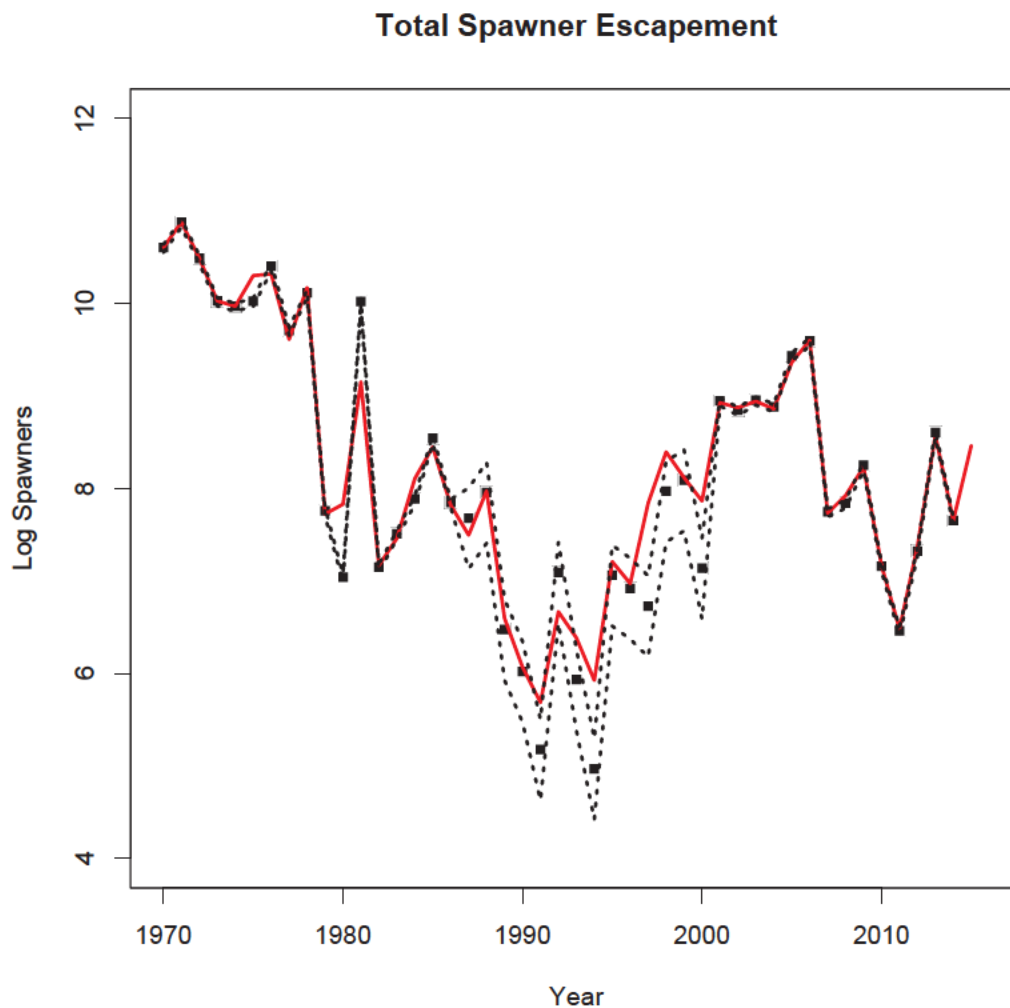


Figure 15. Model fit (red line) to log natural origin escapement data (squares) with 95% interval on measurement error (dashed lines).

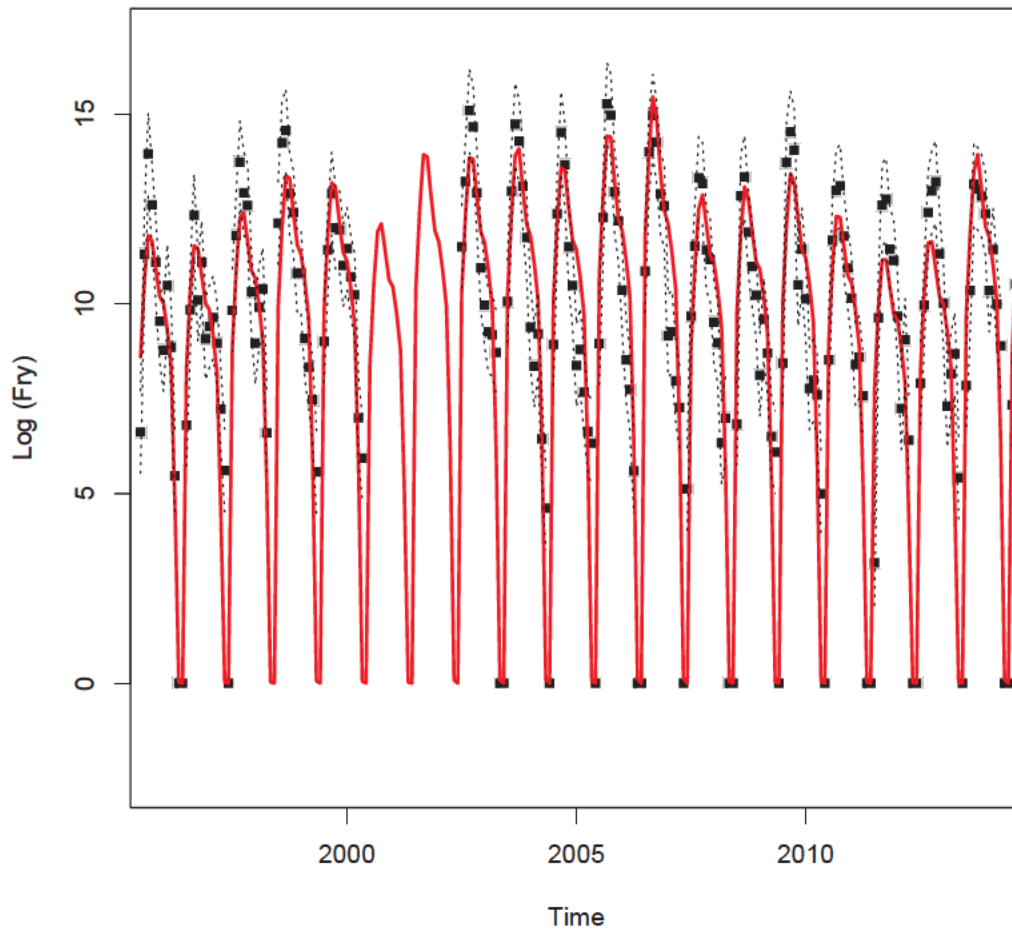


Figure 16. Model fit (red line) to monthly juvenile abundance estimates at Red Bluff Diversion Dam from 1996 to 2014 (squares) with 95% interval on measurement error (dashed lines).

Catches at Knights Landing were estimated by applying the proportion of fish predicted by the model to the observed total catches in a given year. The WRLCM used the flow triggers at Wilkins Slough (Rearing transition) of greater than $400 \text{ m}^3\text{s}^{-1}$ to move fish past Knights Landing, and the model was able to capture the general patterns in movement among years as a function of the flow trigger (Figure 17 and 18).

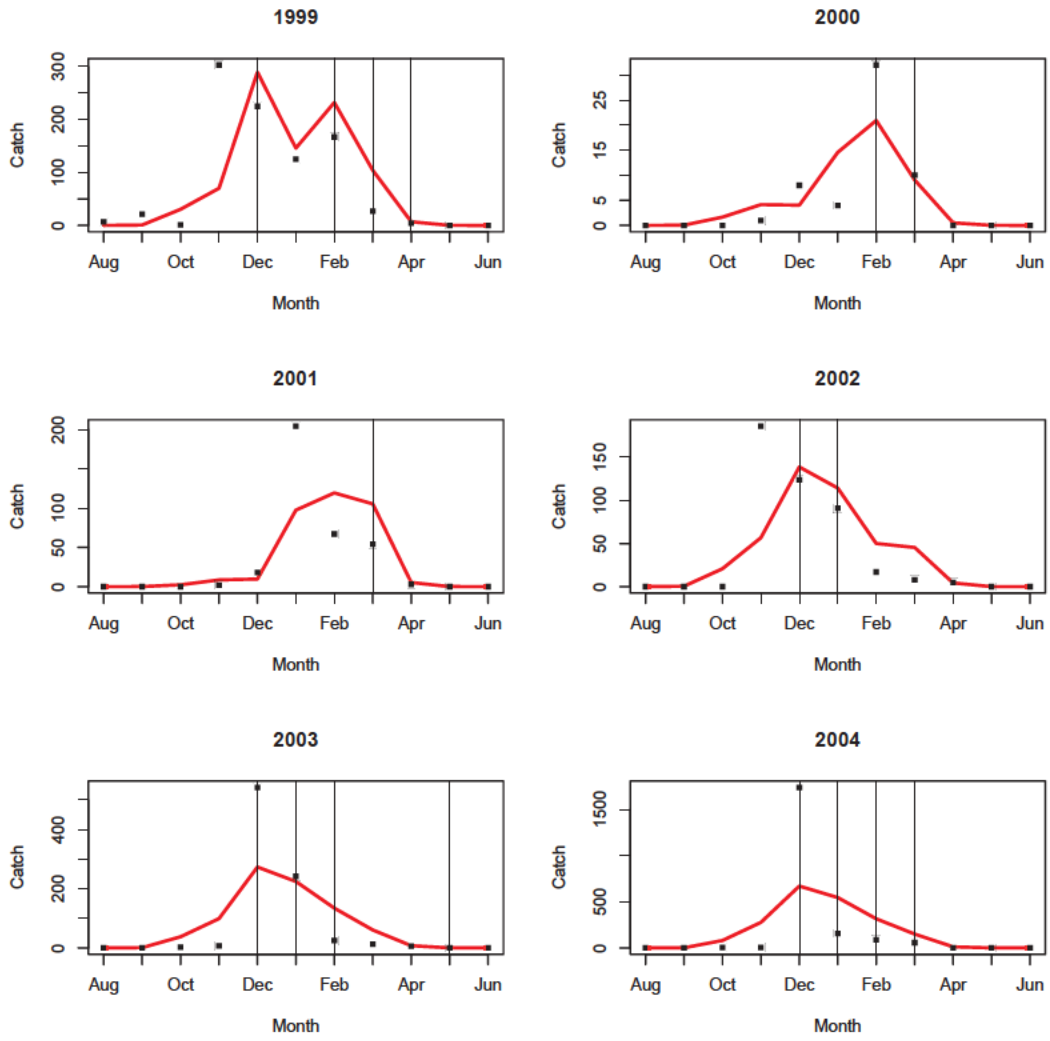


Figure 17. Model fits (red line) to Knights Landing catch data (black squares) from 1999 to 2004. Vertical lines indicate months in which the average flow at Wilkins Slough was greater than $400 \text{ m}^3 \text{ s}^{-1}$.

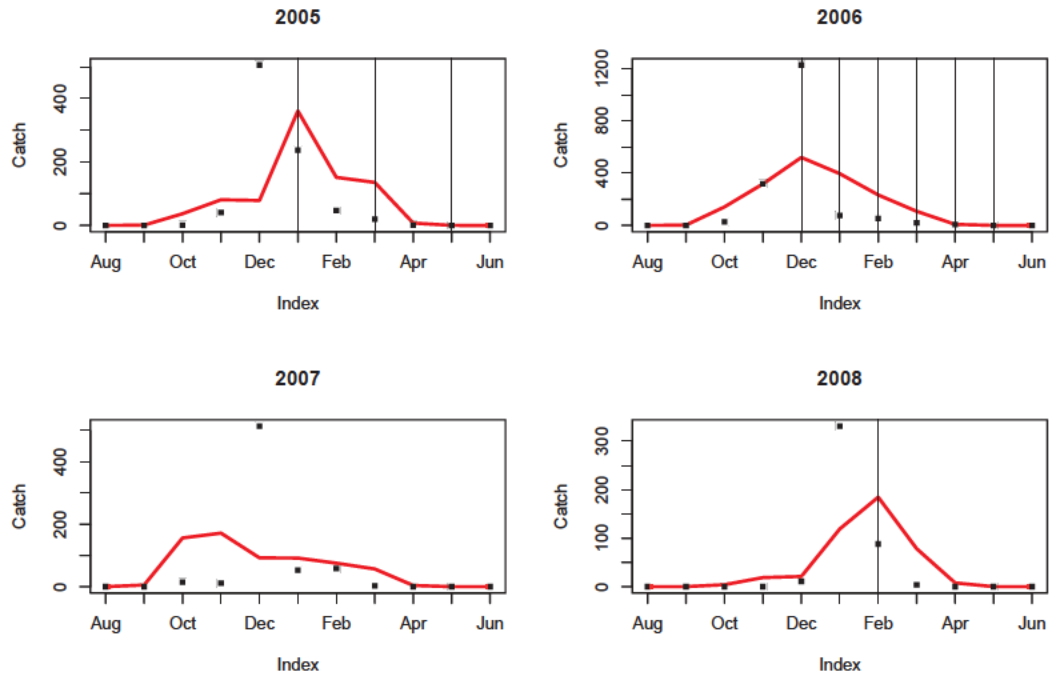


Figure 18. Model fits (red line) to Knights Landing catch data (black squares) from 2005 to 2008. Vertical lines indicate months in which the average flow at Wilkins Slough was greater than $400 \text{ m}^3 \text{ s}^{-1}$.

Finally, the WRLCM was able to capture the monthly patterns in Chipps Island abundance trends from 2008 – 2011, reflecting the outmigration patterns of winter-run from each of the rearing habitats (Figure 19).

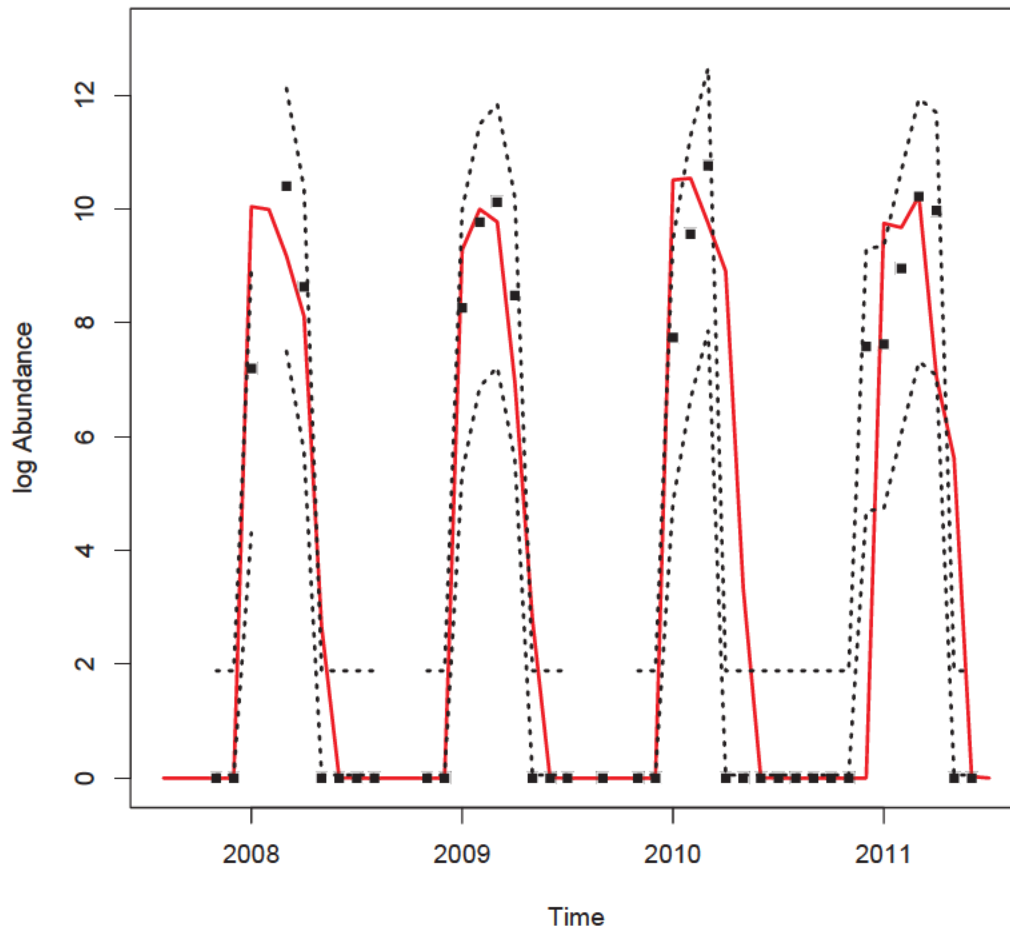


Figure 19. Model fits (red line) to monthly Chipps Island abundance estimates (black squares) from 2008 to 2011 with 95% interval on measurement error (dashed lines).

The estimated parameter values from the Expectation-Maximization algorithm are provided in Table 7. The table provides the parameter estimate, the standard deviation of the estimate (SD), a transformed value of the parameter estimate, and a note defining the parameter. We attempted to estimate all parameters of the survival of egg to fry as a function of temperature (Transition 1); however, there was strong correlation among the three parameters that caused problems with parameter identifiability. We assumed that the survival rate from egg to fry in the absence of thermal mortality was 0.321, which is consistent with historical estimates of egg to fry survival values (Poytress et al. 2014). The parameter estimates indicated that the 3-month trailing average (spawn month and trailing 2 months) of 13.4 °C (*t.crit*) was thermal threshold. Above the thermal threshold, the survival of egg to fry below this critical temperature the survival was 0.321 ($B0_1$) for the 3-month period, whereas above this threshold the survival was reduced ($B1_1$).

The other parameter value that was set was the variance on the random effect in process noise (σ_{ε^2}), and it was set to have a value of 1. This variance allowed the model to estimate the annual random effect parameters (ε_t) to have values of approximately ± 2 . These parameter values corresponded to a range in annual variability in survival of (0.17, 7.4) due to the lognormal structure of the random effects.

Table 7. WRLCM parameter estimates from the model calibration to winter-run indices of abundance (Table 6).

| Parameter | Estimate | SD | Transformed | |
|----------------------------|----------|--------|-------------|---|
| | | | Value | Notes |
| t_{crit} | 13.4 | 0.0521 | 13.4 | Critical temperature (C) at which egg to fry survival is reduced |
| $B0_1^*$ | -0.75 | 0 | 0.321 | Survival below critical temperature value (logit space) |
| $B1_1$ | -0.785 | 0.0213 | NA | Rate of reduction in egg to fry survival (logit space) |
| S_{FRY} | 1.25 | 0.0338 | 0.777 | Winter run fry survival (logit space) |
| mig_{LH} | -0.604 | 0.0423 | 0.268 | Proportion of fry in upper river migrating to lower river per month (logit space) |
| $B0_M$ | -5.56 | 0.815 | 0.001 | Wilkins slough movement without trigger (logit space) |
| $B1_M$ | 4.95 | 0.819 | NA | Wilkins slough change in movement with flow trigger (logit space), proportion moving with flow effect is 0.35 |
| $B1_{10}$ | 1.47 | 0.0526 | NA | River smolt survival from flow effect |
| S_{G1} | -1.68 | 0.0441 | 0.157 | Gulf entry for upper river, lower river, and floodplain |
| $\sigma_{\varepsilon^2}^*$ | 1 | 0 | | Variance of annual random effects in process noise |

* parameters fixed in estimation but are relevant for the estimation portion of the model

Using the Hessian matrix (second derivative of parameter estimates with respect to the likelihood surface at the maximum likelihood estimate), we were able to calculate the Fisher information matrix, and obtain estimates of the standard deviation of the model parameters (Table 7) and the correlation among estimated model parameters (Table 8). Several parameters had high correlations. The estimated parameters of the egg to fry survival (Transition 1) had a strong negative correlation (-0.79). In addition, the parameters of the fry movement function from the

Lower River to the Delta (Rearing transition) as a function of Wilkins Slough flow had a high positive correlation (0.99). Finally, the survival at ocean entry was negatively correlated with the fry survival rate (-0.96) and the critical temperature (-0.68).

Table 8. Correlation matrix for estimated parameters in the WRLCM calibration.

| | <i>t.crit</i> | <i>B1₁</i> | <i>S_{FRY}</i> | <i>mig_{LH}</i> | <i>B0_M</i> | <i>B1_M</i> | <i>B1₁₀</i> | <i>S_{G1}</i> |
|-------------------------|---------------|-----------------------|------------------------|-------------------------|-----------------------|-----------------------|------------------------|-----------------------|
| <i>t.crit</i> | 1 | -0.79 | 0.56 | 0.33 | -0.02 | -0.05 | 0.01 | -0.68 |
| <i>B1₁</i> | -0.79 | 1 | -0.55 | -0.46 | 0.03 | 0 | -0.41 | 0.55 |
| <i>S_{FRY}</i> | 0.56 | -0.55 | 1 | 0.26 | 0.08 | -0.09 | 0.18 | -0.96 |
| <i>mig_{LH}</i> | 0.33 | -0.46 | 0.26 | 1 | 0.04 | -0.04 | 0.41 | -0.25 |
| <i>B0_M</i> | -0.02 | 0.03 | 0.08 | 0.04 | 1 | -0.99 | 0.03 | -0.01 |
| <i>B1_M</i> | -0.05 | 0 | -0.09 | -0.04 | -0.99 | 1 | 0 | 0.05 |
| <i>B1₁₀</i> | 0.01 | -0.41 | 0.18 | 0.41 | 0.03 | 0 | 1 | 0.01 |
| <i>S_{G1}</i> | -0.68 | 0.55 | -0.96 | -0.25 | -0.01 | 0.05 | 0.01 | 1 |

Developing parameter sets for Monte Carlo simulations

To compare alternative hydromanagement actions, Monte Carlo simulations should be run under each of the actions. We have obtained estimates of parameter uncertainty and correlation in the model calibration from the Hessian matrix (Table 8) to incorporate into the Monte Carlo simulation. For those parameters that were estimated, Monte Carlo parameter values were drawn from multivariate normal distribution centered on the maximum likelihood estimates (MLE) and using the covariance matrix estimated from the Hessian obtained at the MLE. The draws from the multivariate normal distribution incorporated the relative uncertainty in the estimated parameters and preserved the strong correlation among several of the life cycle model parameters that were identified in the correlation matrix of the parameter estimates (Table 7). For the random effects, iid normal $N(0,1)$ random variables were drawn to reflect the annual random effects in the process noise. All other parameters were set to their fixed values as described above. Please see Appendix B for a list of all parameter values.

V. References

- Anderson, J., Gurarie, E., and Zabel, R. 2005. Mean free-path length theory of predator-prey interactions: Application to juvenile salmon migration. *Ecological Modeling*, 186, 196-211.
- Anderson, J., and Mierzwa, M. 2002. An introduction to the Delta Simulation Model II (DSM2) for simulation of hydrodynamics and water quality of the Sacramento-San Joaquin Delta, Delta Modeling Section, Office of State Water Project Planning, California Department of Water Resources, Sacram., Ca.
- Beamer, E., A. McBride, C. Greene, R. Henderson, G. Hood, K. Wolf, K. Larsen, C. Rice, and K. L. Fresh. 2005. Delta and nearshore restoration for the recovery of wild Skagit River Chinook salmon: Linking estuary restoration to wild Chinook salmon populations. Appendix D of the Skagit Chinook Recovery Plan, Skagit River System Cooperative, LaConner, WA. Available at: www.skagitcoop.org.
- Bay Delta Conservation Plan. 2013. *Modeling Technical Appendix*, EIR/EIS Report.
- Björnsson, B. T., S. O. Stefansson, and S. D. McCormick. 2011. Environmental endocrinology of salmon smoltification. *General and Comparative Endocrinology* 170(2):290-298.
- Chapman, E.D., Hearn, A.R., Michel, C.J., Ammann, A.J., Lindley, S.T., Thomas, M.J., Philip T. Sandstrom, P.T., Singer, G.P., Peterson, M.L., MacFarlane, R.B., and Klimley, A.P. 2013. Diel movements of out-migrating Chinook salmon (*Oncorhynchus tshawytscha*) and steelhead trout (*Oncorhynchus mykiss*) smolts in the Sacramento/San Joaquin watershed. *Environ. Biol. Fishes*, 96(2-3), 273-286.
- DeLong, L.L., Lewis, L., Thompson, D.B., and Lee, J.K. 1997. The computer program FourPt (Version 95.01): A model for simulating one -dimensional, unsteady, open-channel flow, Water-Resources Investigation Report, 97-4016, USGS, Branch of Information Services.
- del Rosario, R. B., Y. J.Redler., K. Newman, P. L. Brandes, T. Sommer, K. Reece, and R. Vincik. 2013. Migration patterns of juvenile winter-run-sized Chinook salmon (*Oncorhynchus tshawytscha*) through the Sacramento–San Joaquin Delta. *San Francisco Estuary and Watershed Science* 11(1).
- Dempster, A.P.; Laird, N.M.; Rubin, D.B. 1977. Maximum likelihood from incomplete data via the EM algorithm. *Journal of the Royal Statistical Society, Series B.* 39 (1): 1–38.
- Gibson, R.N., 2003. Go with the flow: tidal migration in marine animals, In *Migration and Dispersal of Marine Organisms*, 153-161, Springer, Netherlands.
- Greene, C.M., D.W. Jensen, E. Beamer, G.R. Pess, and E.A. Steel. 2005. Effects of environmental conditions during stream, estuary, and ocean residency on Chinook salmon return rates in the Skagit River, WA. *Transactions of the American Fisheries Society*, 134:1562-1581.
- Grover, A., A. Lowe, P. Ward, J. Smith, M. Mohr, D. Viele, and C. Tracy. 2004. Recommendations for developing fishery management plan conservation objectives for Sacramento River winter Chinook and Sacramento River spring Chinook. Interagency Workgroup Progress Report. February 2004.

- Hastie, T.J., R.J. Tibshirani, R.J. and J.H. Friedman. 2001. The elements of statistical learning: data mining, inference, and prediction. Springer.
- Hendrix, N., Criss, A., Danner, E., Greene, C.M., Imaki, H., Pike, A., and Lindley, S.T. 2014. Life cycle modeling framework for Sacramento River Winter run Chinook salmon, NOAA Technical Memorandum 530, National Marine Fisheries Service, Southwest Fisheries Science Center, Santa Cruz, Ca.
- Hilborn, R. and M. Mangel. 1997. The ecological detective: confronting models with data. Princeton University Press.
- Hood, W.G. 2007. Landscape allometry and prediction in estuarine ecology: Linking landform scaling to ecological patterns and processes. *Estuaries and Coasts*, 30: 895-900.
- Jassby, A. D., W.J. Kimmerer, S.G. Monismith, C. Armor, J.E. Cloern, T.M. Powell, J.R. Schubel, and T.J. Vendlinski. 1995. Isohaline position as a habitat indicator for estuarine populations. *Ecological Applications* 5: 272-289.
- Jackson, D., Perry, R., Pope, A., Wang, X., Lindley, S., Sridharan, V., and Freidman, W. 2016. An agent-based model of Chinook salmon migration in the Sacramento-San Joaquin Delta. In prep.
- Kimmerer, W.J., and Nobriga, M.L. 2008. Investigating particle transport and fate in the Sacramento-San Joaquin Delta using a particle tracking model. *San Francisco Estuary Watershed Sci.*, 6(1).
- Kundu, P. K., and Cohen, I. M. 2002. Fluid Mechanics. 2nd Edition. Academic Press.
- Liao, J. 2007. A review of fish swimming mechanics and behavior in altered flows. *Phil. Trans. Royal Soc. B: Biol. Sci.*, 362(1487), 1973–1993.
- Monismith, S.G., W. Kimmerer, J.R. Burau, and M.T Stacey. 2002. Structure and flow-induced variability of the subtidal salinity field in northern San Francisco Bay. *Journal of Physical Oceanography*, 32: 3003-3019.
- Neal, R. and G. Hinton. 1999. A view of the EM algorithm that justifies incremental, sparse, and other variants. Pages 355–368 *Learning in Graphical Models*, Michael I. Jordan, ed. MIT Press.
- National Marine Fisheries Service (NMFS) 2012. Final Implementation of the 2010 Reasonable and Prudent Alternative Sacramento River winter-run Chinook Management Framework for the Pacific Coast Salmon Fishery Management Plan. National Marine Fisheries Service, Southwest Region.
- Newman, K., S.T. Buckland, B. Morgan, R. King, D.L. Borchers, D. Cole, P. Besbeas, O. Gimenez, and L. Thomas. 2014. *Modelling population dynamics*. Springer.
- O'Farrell, M. R., M. S. Mohr, A. M. Grover, and W. H. Satterthwaite. 2012. Sacramento River winter Chinook cohort reconstruction: analysis of ocean fishery impacts. NOAA Technical Memorandum NOAA-TM-NMFS- SWFSC-491.
- O'Farrell, M. and W. H. Satterthwaite. 2015. Inferred historical fishing mortality rates for an endangered population of Chinook salmon (*Oncorhynchus tshawytscha*). *Fishery Bulletin*, 113(3):341-352.

Poytress, W. R., J. J. Gruber, F. D. Carrillo and S. D. Voss. 2014. Compendium Report of Red Bluff Diversion Dam Rotary Trap Juvenile Anadromous Fish Production Indices for Years 2002-2012. Report of U.S. Fish and Wildlife Service to California Department of Fish and Wildlife and US Bureau of Reclamation.

Prandtl, L. 1935. The mechanics of viscous fluids, In *Aerodynamic Theory*, Ed. Durand W.F., 3, 34-208.

R Core Development Team (RCDT). 2016. R: A language and environment for statistical computing. R Foundation for Statistical Computing, Vienna, Austria. URL <https://www.R-project.org/>.

Semmens, B. X. 2008. Acoustically derived fine-scale behaviors of juvenile Chinook salmon (*Oncorhynchus tshawytscha*) associated with intertidal benthic habitats in an estuary. *Canadian Journal of Fisheries and Aquatic Sciences*, 65: 2053-2062.

Sridharan, V.K., Jackson, D., Friedman, W., Perry, R., Pope, A., Wang, X., Lindley, S.T., Danner, E. and Monismith, S.G. Physical mechanisms governing fates of salmon transiting an urban estuary. In prep.

U.S. Bureau of Reclamation. 2003. Hydro24ca - Selected hydrologic features 1:24,000-scale for California. http://projects.atlas.ca.gov/frs/?group_id=39&release_id=23

U.S. Fish and Wildlife Service. 2007. 2001-2005 annual progress report: "Abundance and survival of juvenile chinook salmon in the Sacramento-San Joaquin Estuary". Stockton, CA. https://www.fws.gov/lodi/juvenile_fish_monitoring_program/jfmp_reports.htm

Visser, A. 1997. Using random walk models to simulate the vertical distribution of particles in a turbulent water column. *Mar. Ecol. Prog. Ser.*, 158, 275-281.

Wang, B., Fringer, O. B., Giddings, S. N., and Fong, D. A. 2009. High-resolution simulations of a macrotidal estuary using SUNTANS. *Ocean Modell.*, 28(1), 167-192.

Wilbur R. 2000. Validation of dispersion using the particle tracking model in the Sacramento-San Joaquin Delta. Masters Thesis, University of California, Davis, Ca.

Winship, A.J., M.R. O'Farrell and M.S. Mohr. 2014. Fishery and hatchery effects on an endangered salmon population with low productivity. *Transactions of the American Fisheries Society*, 143(4):957-971.

Appendix A. Analysis of winter-run monthly spawn timing

To estimate the proportion of winter-run spawning among the months of April to August, we conducted an analysis of the numbers of winter-run carcasses detected in each of the months April to August. We were interested in understanding whether the proportions spawning among months were static across all years, or alternatively, whether the proportions varied among years due to the environmental conditions in that year. That is, whether there were some environmental conditions that caused shifts to earlier spawning in some years.

Data

Winter-run carcass observations by date were shifted two weeks earlier to generate “observed” number of fish spawning by date. These spawning numbers by date were coalesced by month to form $N.spawn_{m,t}$ the observed (based on carcass counts) number of winter-run Chinook spawning in month m in year t .

To evaluate annual variability in the proportion spawning in a given month, we calculated a spawning proportion anomaly as the standardized proportion of fish spawning each month ($SP_{m,t}$). For example, the values of the standardized April values were

$$SP_{Apr,t} = \frac{P.spawn_{Apr,t} - \text{mean}(P.spawn_{Apr})}{\text{std dev}(P.spawn_{Apr})}$$

where the proportion spawning in each month for a given year t (subscript suppressed) was calculated as

$$P.spawn_m = \frac{N.spawn_m}{\sum_m N.spawn_m}$$

To understand how these annual anomalies varied as a function of water temperature, we calculated the Pearson’s correlation coefficient between mean monthly temperature below Keswick Dam between January and June and the standardized proportions (Figure A1).

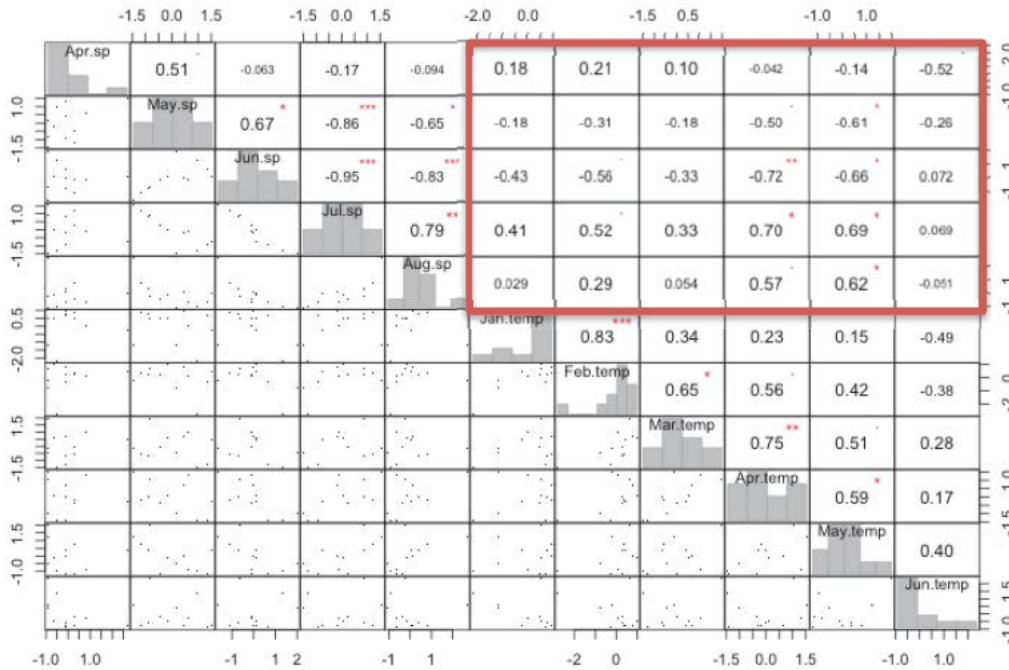


Figure A1. Pearson correlation coefficients (upper triangle), histograms (diagonal) and scatter plots (lower triangle) for all combinations of monthly spawning proportion anomalies and Keswick water temperatures. The red box indicates the month by temperature correlations, and red asterisks indicate significant correlation coefficients.

Statistical analysis

We fit a multinomial logistic regression using the *multinom* function from the *nnet* package in R to the number of winter-run Chinook spawning in each month, $N.spawn_{m,t}$. We evaluated the ability of April Keswick temperatures to explain annual variability in the spawning timing. We focused on April temperatures because April is the first month of spawning, and April would allow this physical variable to be used as a predictor of spawn timing for future years. The monthly average April temperatures at Keswick were standardized (subtracted mean and divided by standard deviation) for use in the multinomial model.

We fit a base model without the April temperature effect and we fit the model with the April effect and used Akaike Information Criterion (AIC) to compare the models. The AIC value for the base multinomial model was 75822, whereas the value for the multinomial model including April temperature as a covariate was 74209. The difference in AIC was 1613, providing strong support for the model with the April temperature covariate.

The model coefficients for the multinomial model with April covariate indicated increasing spawning in July and August (positive coefficient values) when April temperatures increased (Table A1 and Figure A2). The model coefficients (Table A1) can thus be used for making predictions of spawning proportions using standardized April temperatures as displayed in Figure A2.

Table A1. Coefficient estimates of the multinomial model including April covariate. The effect of the April covariate is reflected in the B1 coefficient estimate.

| Month | Estimate | | Standard Error | |
|-------|----------|--------|----------------|-------|
| | B0 | B1 | B0 | B1 |
| Apr | -4.145 | 0.054 | 0.06 | 0.062 |
| May | -1.796 | -0.203 | 0.02 | 0.02 |
| Jul | -0.332 | 0.385 | 0.012 | 0.012 |
| Aug | -3.443 | 0.792 | 0.044 | 0.045 |

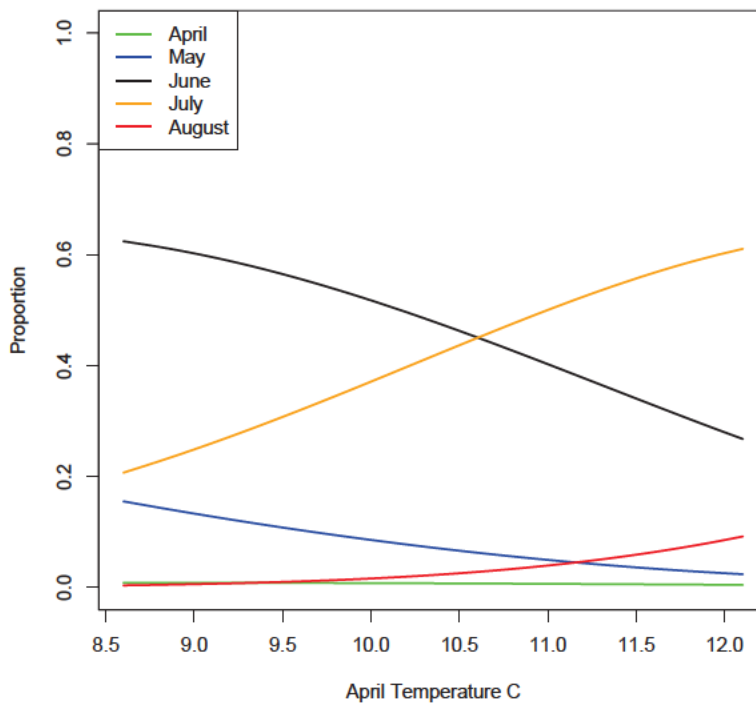


Figure A2. Predictions of the proportion of winter-run Chinook spawning from the multinomial regression model using April temperatures at Keswick Dam as a predictor variable.

Appendix B. Table of parameter values for WRLCM

Table B1. Parameter values, standard deviation (SD), transformed values, transition numbers in which parameters are found and brief description of parameter.

| Name | Value | SD* | Transformed | | Description |
|-----------------------------|--------|-------|-------------|------------|--|
| | | | Value | Transition | |
| <i>t.crit</i> | 13.40 | 0.052 | 13.40 | 1 | Critical temperature (C) at which egg to fry survival is reduced |
| <i>BO₁</i> | -0.75 | 0 | 0.236 | 1 | Survival below critical temperature value (logit space) |
| <i>B1₁</i> | -0.785 | 0.021 | NA | 1 | Rate of reduction in egg to fry survival (logit space) |
| <i>P_{TF,m}</i> | -3 | 0 | 0.047 | 2 | Proportion tidal fry |
| <i>S_{TF,FP}</i> | 1 | 0 | 0.731 | 3 | Survival tidal fry in floodplain |
| <i>min.p</i> | 0.05 | 0 | 0.05 | 3 | Minimum proportion entering Yolo bypass under flow < 100 cfs |
| <i>p.rate</i> | 1.1 | 0 | NA | 3 | Rate of increase in proportion entering Yolo bypass for flows > 6000 cfs |
| <i>BO₄</i> | 0 | 0 | 0.5 | 4 | Average survival tidal fry to delta intercept |
| <i>B1₄</i> | -1 | 0 | NA | 4 | Effect of DCC gate (value is in logit space)* |
| <i>BO₅</i> | 0 | 0 | 0.5 | 5 | Average proportion of tidal fry to bay intercept |
| <i>B1₅</i> | 2 | 0 | NA | 5 | Proportion tidal fry to bay - flow at Rio Vista effect |
| <i>S_{TF,DE-BA}</i> | -1 | 0 | 0.269 | 5 | Survival of tidal fry from delta to bay |
| <i>S_{FRY}</i> | 1.25 | 0.034 | 0.777 | Rearing | Winter run fry survival |
| <i>mig_{LH}</i> | -0.604 | 0.042 | 0.268 | Rearing | Proportion of fry in upper river migrating to lower river per month |
| <i>BO_M</i> | -5.56 | 0.815 | 0.001 | Rearing | Wilkins slough movement without trigger |
| <i>B1_M</i> | 4.95 | 0.819 | NA | Rearing | Wilkins slough change in movement with flow trigger, movement rate under flow trigger is 0.352 |
| <i>mig</i> | -3 | 0 | 0.047 | Rearing | Probability of migration from habitats |
| <i>S_{FRY,BA}</i> | -7 | 0 | 0.001 | Rearing | Survival of bay rearing fry pushed to gulf |
| <i>Z₁</i> | -1 | 0 | 0.269 | 11 to 15 | January smolt probability |
| <i>Z₂</i> | 0 | 0 | 0.5 | 11 to 15 | February smolt probability |
| <i>Z₃</i> | 3 | 0 | 0.953 | 11 to 15 | March smolt probability |

| Name | Value | SD* | Transformed | | Description |
|---------------------|--------|-------|-------------|------------|--|
| | | | Value | Transition | |
| Z_4 | 8 | 0 | 1 | 11 to 15 | April smolt probability |
| Z_5 | 10 | 0 | 1 | 11 to 15 | May smolt probability |
| Z_6 | 10 | 0 | 1 | 11 to 15 | June smolt probability |
| Z_7 | 10 | 0 | 1 | 11 to 15 | July smolt probability |
| $BO_{11,LR}$ | 1.39 | 0 | 0.801 | 12 | Smolt survival lower river to delta |
| $BO_{10,UR}$ | -0.4 | 0 | 0.401 | 11 | Survival of upper river fish to lower river |
| $B1_{10}$ | 1.47 | 0.053 | NA | 11,12 | River smolt survival from flow effect |
| $^cS_{11}$ | 1.5 | 0 | 0.818 | 11 to 14 | Survival smolt chipps to ocean - assume 0.8 |
| $^AS_{13,FP,m}$ | 2.5 | 0 | 0.924 | 13 | survival from Yolo until Delta, assume 0.92 (at least until insertion point into PTM in Delta) |
| $S_{15,BA}$ | 0 | 0 | 0.5 | 15 | Survival of smolts bay to ocean |
| S_{G1} | -1.68 | 0.044 | 0.157 | 11, 12, 13 | Gulf entry for upper river, lower river, and floodplain |
| D_{G2} | -0.5 | 0 | NA | 14, 15 | Gulf entry decrement for delta and bay (value in logit space) |
| σ_ϵ^2 | 1 | 0 | 1 | | Variance of annual random effects in process noise |
| S_{17} | 1.35 | 0 | 0.794 | 17, 18 | Probability of survival age 1 to age 2 over 4 months |
| M_2 | -2.2 | 0 | 0.1 | 17,18 | Probability of maturation age 2 |
| S_{sp2} | 2.2 | 0 | 0.9 | 18 | Survival ocean exit to spawning ground age 2 |
| S_{19} | 1.4 | 0 | 0.802 | 19 | Probability of survival age 2 to age 3 |
| M_3 | 2.2 | 0 | 0.9 | 19, 20 | Conditional probability of maturation at age 3 |
| S_{sp3} | 2.2 | 0 | 0.9 | 20 | Survival ocean exit to spawning ground age 3 |
| S_{21} | 1.4 | 0 | 0.802 | 21 | Survival age 3 to age 4 |
| S_{sp4} | 2.2 | 0 | 0.9 | 21 | Survival ocean exit to spawning ground age 4 |
| $V_{eggs,2}$ | 3200 | 0 | 3200 | 22 | Eggs per spawner age 2 |
| $V_{eggs,3}$ | 5000 | 0 | 5000 | 22 | Eggs per spawner age 3 |
| $V_{eggs,4}$ | 5000 | 0 | 5000 | 22 | Eggs per spawner age 4 |
| BO_{Apr} | -4.145 | 0 | NA | 22 | Intercept for proportion of spawners in April |

| Name | Value | SD* | Transformed | | Description |
|---------------------------|---------|-----|-------------|------------|---|
| | | | Value | Transition | |
| <i>B1_{Apr}</i> | 0.0538 | 0 | NA | 22 | Effect of temperature on proportion of spawners in April |
| <i>B0_{May}</i> | -1.796 | 0 | NA | 22 | Intercept for proportion of spawners in May |
| <i>B1_{May}</i> | -0.2031 | 0 | NA | 22 | Effect of temperature on proportion of spawners in May |
| <i>B0_{Jul}</i> | -0.332 | 0 | NA | 22 | Intercept for proportion of spawners in July |
| <i>B1_{Jul}</i> | 0.3852 | 0 | NA | 22 | Effect of temperature on proportion of spawners in July |
| <i>B0_{Aug}</i> | -3.443 | 0 | NA | 22 | Intercept for proportion of spawners in August |
| <i>B1_{Aug}</i> | 0.7921 | 0 | NA | 22 | Effect of temperature on proportion of spawners in August |
| <i>Fem_{Age2}</i> | 0.01 | 0 | 0.01 | 18 | Proportion of age 2 spawners that are female |
| <i>Fem_{Age3}</i> | 0.5 | 0 | 0.5 | 20 | Proportion of age 3 and 4 that are female |
| <i>K_{Sp,m}</i> | 50000 | 0 | 50000 | 22 | Capacity in the spawning reaches by month |

*Estimated parameter values have associated standard deviations (SD)